

Highlights from PIC simulations of ultraintense laser-plasma interactions

Andrea Macchi

www.df.unipi.it/~macchi

polyLAB, CNR-INFM, and INFN, sezione di Pisa,
Dipartimento di Fisica “E. Fermi”, Università di Pisa, Italy



CSFI 2008 Conference, Rimini, May 29, 2008

Coworkers

Coworkers



Tatiana V. Liseykina¹, Alessandra Bigongiari

Department of Physics, University of Pisa, Italy

Coworkers



Tatiana V. Liseykina¹, Alessandra Bigongiari

Department of Physics, University of Pisa, Italy

¹ *On leave from Institute for Computational Technologies, Novosibirsk, Russia*

Presently at Max Planck Institute for Nuclear Physics, Heidelberg, Germany



Coworkers



Tatiana V. Liseykina¹, Alessandra Bigongiari

Department of Physics, University of Pisa, Italy



¹ *On leave from Institute for Computational Technologies, Novosibirsk, Russia*



Presently at Max Planck Institute for Nuclear Physics, Heidelberg, Germany



Collaboration with experimental partners –
Marco Borghesi et al.
*School of Mathematics and Physics,
Queen's University of Belfast, UK*

The speaker acknowledges a visiting fellowship from QUB (presently running)

Outlook

Outlook

- Laser-plasma PIC simulations at CINECA

Outlook

- Laser-plasma PIC simulations at CINECA
- Highlight 1: “coherent” electromagnetic structures in laser plasmas

Outlook

- Laser-plasma PIC simulations at CINECA
- Highlight 1: “coherent” electromagnetic structures in laser plasmas
- Highlight 2: Radiation Pressure Acceleration with circularly polarized pulses

Background and motivations

Background and motivations

- laser-plasma simulation projects running at CINECA almost continuously since 1997 (sponsored by the INFN and CNR/INFN supercomputing initiative)

Background and motivations

- laser-plasma simulation projects running at CINECA almost continuously since 1997 (sponsored by the INFN and CNR/INFN supercomputing initiative)
- simulations mostly based on Lagrangian particle-in-cell (PIC) codes (but also Eulerian “Vlasov” codes, “hybrid” codes, ...)

Background and motivations

- laser-plasma simulation projects running at CINECA almost continuously since 1997 (sponsored by the INFN and CNR/INFN supercomputing initiative)
- simulations mostly based on Lagrangian particle-in-cell (PIC) codes (but also Eulerian “Vlasov” codes, “hybrid” codes, ...)

Topics:

Background and motivations

- laser-plasma simulation projects running at CINECA almost continuously since 1997 (sponsored by the INFN and CNR/INFN supercomputing initiative)
- simulations mostly based on Lagrangian particle-in-cell (PIC) codes (but also Eulerian “Vlasov” codes, “hybrid” codes, ...)

Topics:

- nonlinear dynamics in collisionless, relativistic plasmas

Background and motivations

- laser-plasma simulation projects running at CINECA almost continuously since 1997 (sponsored by the INFN and CNR/INFN supercomputing initiative)
- simulations mostly based on Lagrangian particle-in-cell (PIC) codes (but also Eulerian “Vlasov” codes, “hybrid” codes, ...)

Topics:

- nonlinear dynamics in collisionless, relativistic plasmas
- support to experimental activities

Background and motivations

- laser-plasma simulation projects running at CINECA almost continuously since 1997 (sponsored by the INFN and CNR/INFN supercomputing initiative)
- simulations mostly based on Lagrangian particle-in-cell (PIC) codes (but also Eulerian “Vlasov” codes, “hybrid” codes, . . .)

Topics:

- nonlinear dynamics in collisionless, relativistic plasmas
- support to experimental activities
- “design and feasibility” for future projects (e.g. ELI, HiPER, PLASMONX, . . .)

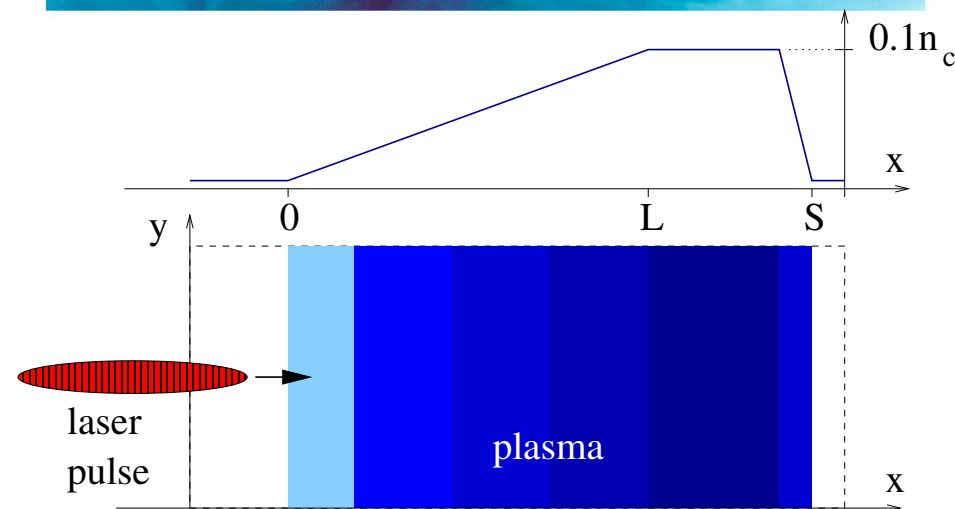
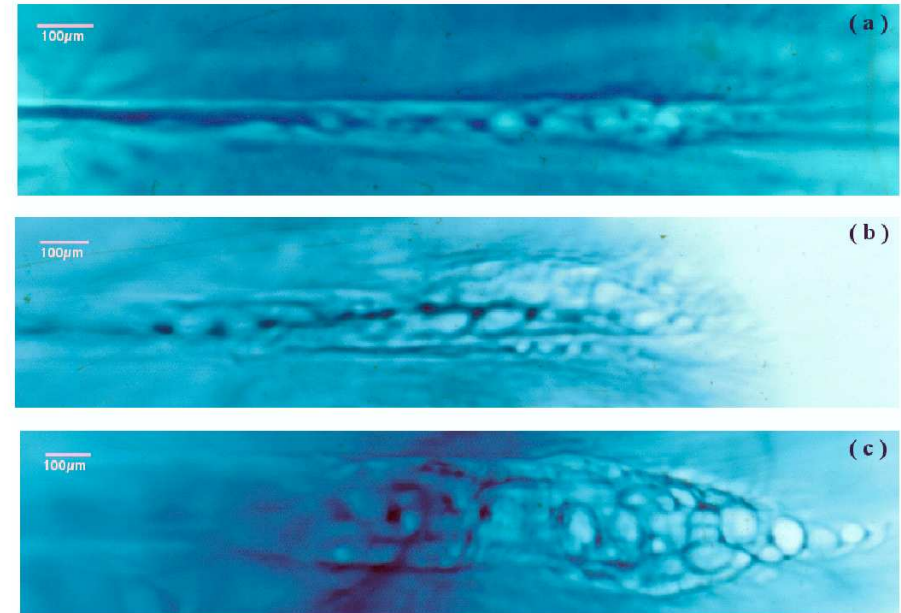
“Coherent” EM structures observed?

Experimental data from the Proton Imaging Technique give evidence of slowly-varying, long-living electric and/or magnetic structures generated by laser-plasma interaction

“Coherent” EM structures observed?

Experimental data from the Proton Imaging Technique give evidence of slowly-varying, long-living electric and/or magnetic structures generated by laser-plasma interaction

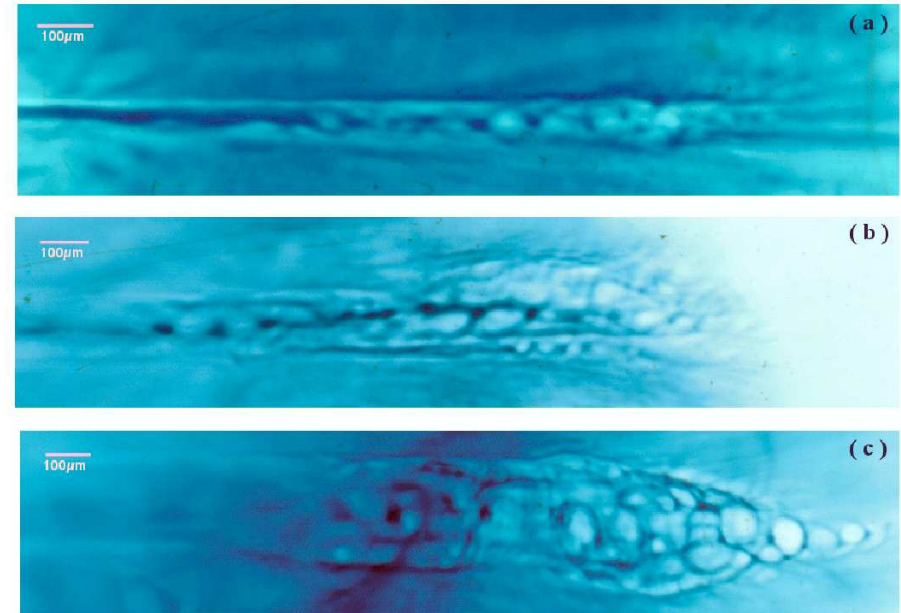
[Kar et al, New J. Phys. **9**, 502 (2007);
Liseikina et al, arXiv:physics/0702177]



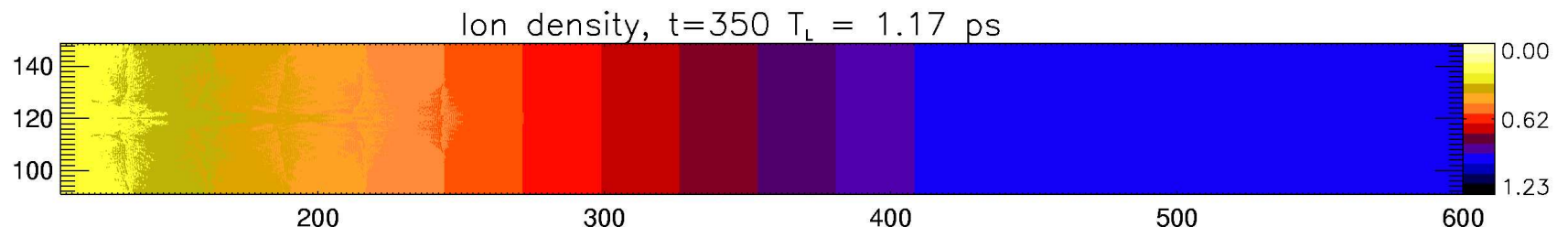
“Coherent” EM structures observed?

Experimental data from the Proton Imaging Technique give evidence of slowly-varying, long-living electric and/or magnetic structures generated by laser-plasma interaction

[Kar et al, New J. Phys. **9**, 502 (2007);
Liseikina et al, arXiv:physics/0702177]



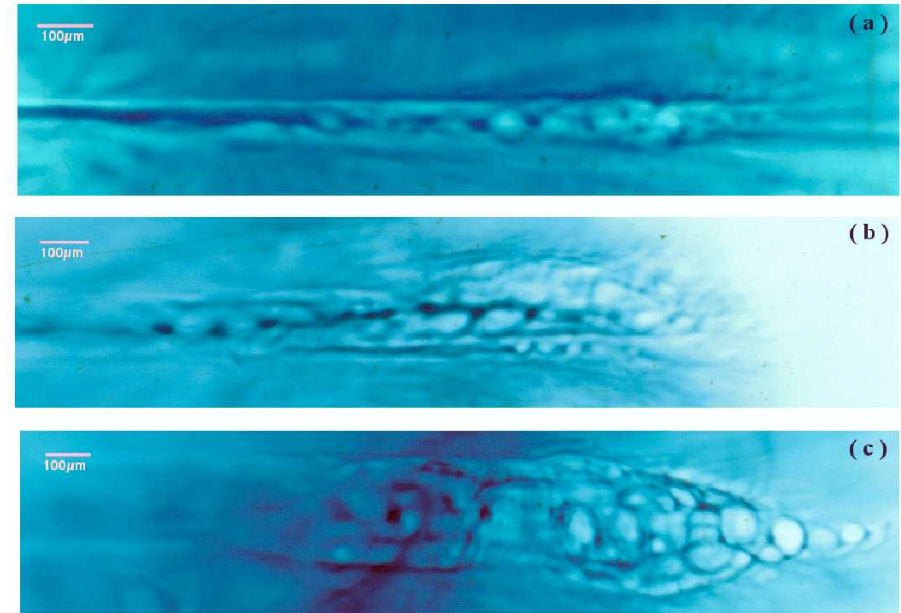
Challenge: make simulations with spatial and temporal scales as close as possible to the experiment



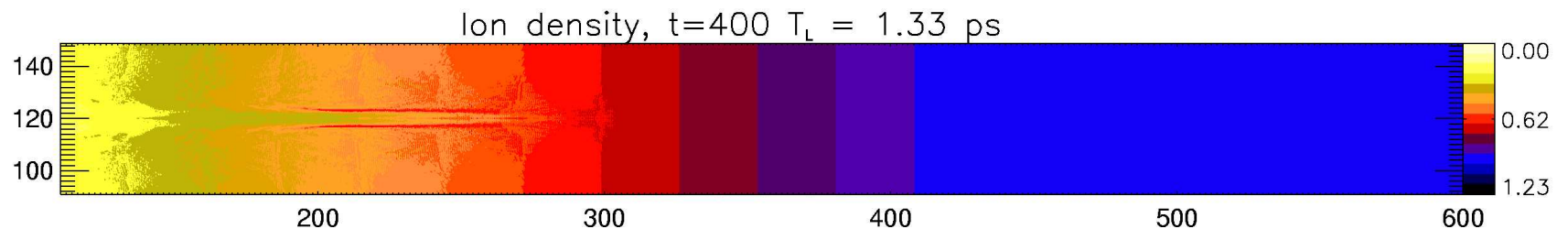
“Coherent” EM structures observed?

Experimental data from the Proton Imaging Technique give evidence of slowly-varying, long-living electric and/or magnetic structures generated by laser-plasma interaction

[Kar et al, New J. Phys. **9**, 502 (2007);
Liseikina et al, arXiv:physics/0702177]



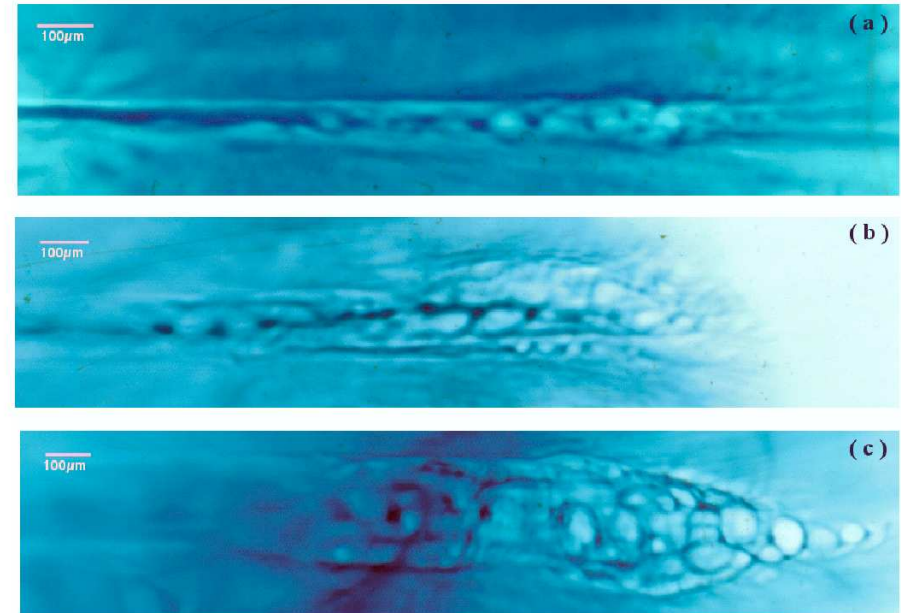
Challenge: make simulations with spatial and temporal scales as close as possible to the experiment



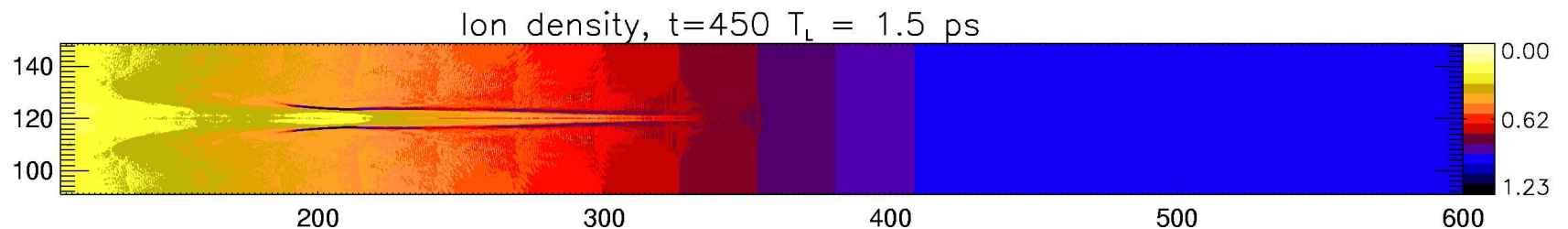
“Coherent” EM structures observed?

Experimental data from the Proton Imaging Technique give evidence of slowly-varying, long-living electric and/or magnetic structures generated by laser-plasma interaction

[Kar et al, New J. Phys. **9**, 502 (2007);
Liseikina et al, arXiv:physics/0702177]



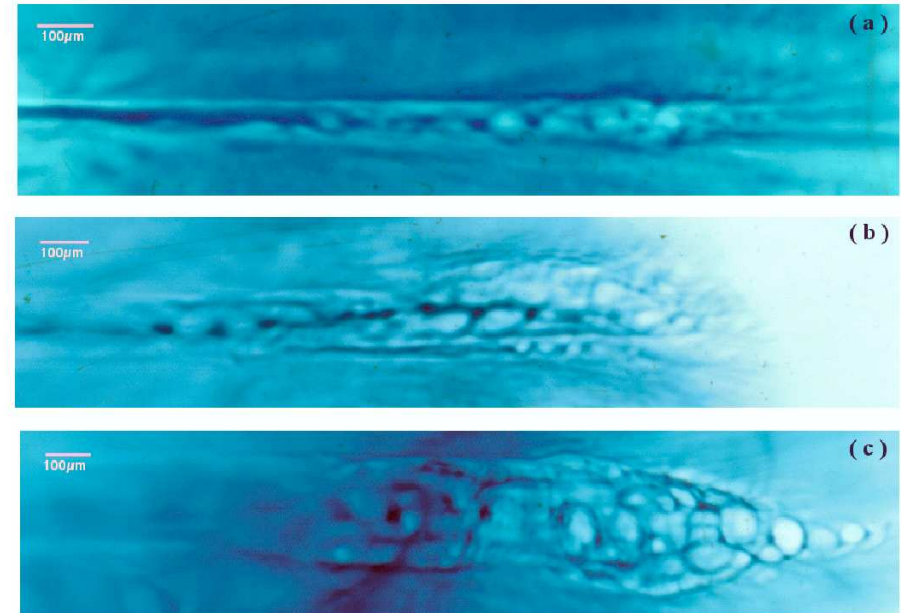
Challenge: make simulations with spatial and temporal scales as close as possible to the experiment



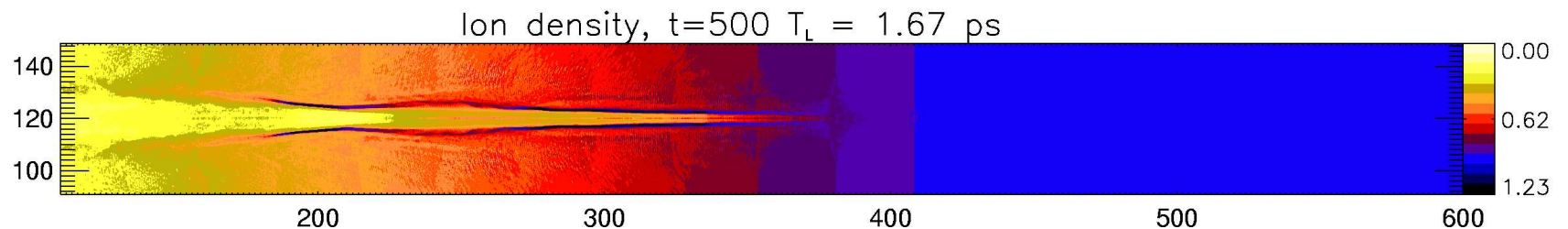
“Coherent” EM structures observed?

Experimental data from the Proton Imaging Technique give evidence of slowly-varying, long-living electric and/or magnetic structures generated by laser-plasma interaction

[Kar et al, New J. Phys. **9**, 502 (2007);
Liseikina et al, arXiv:physics/0702177]



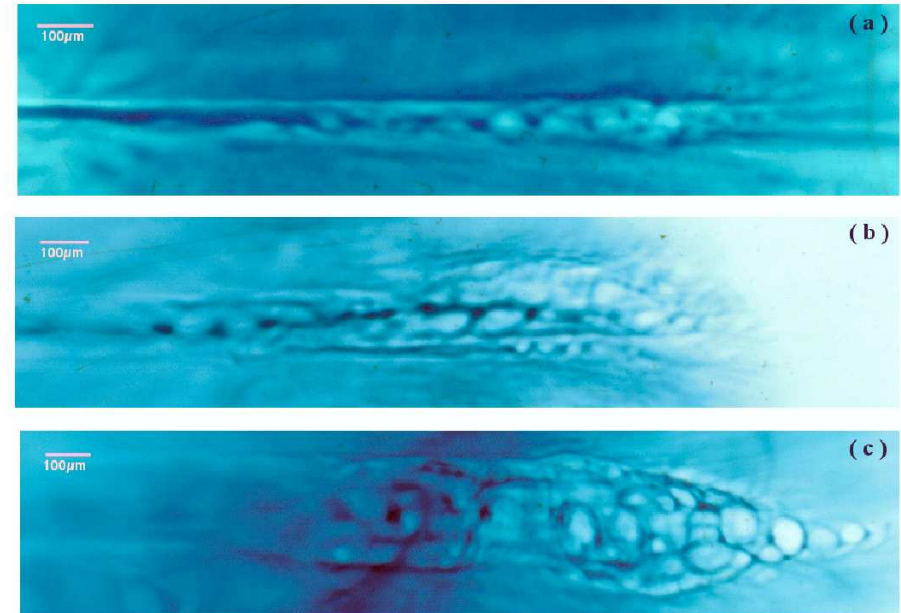
Challenge: make simulations with spatial and temporal scales as close as possible to the experiment



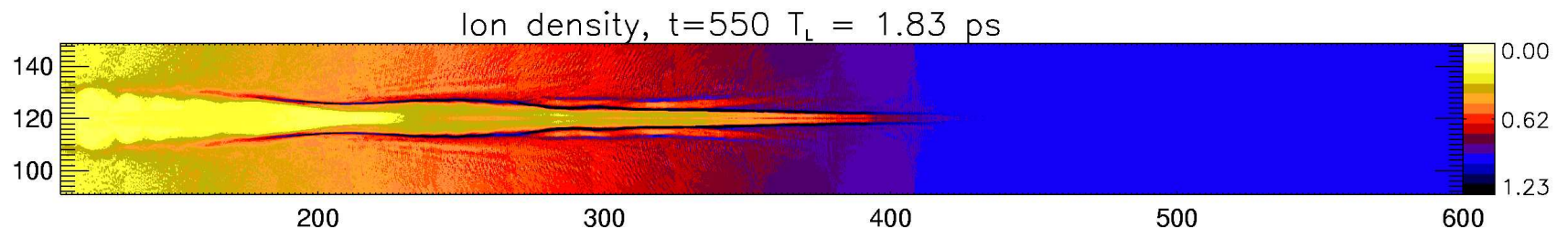
“Coherent” EM structures observed?

Experimental data from the Proton Imaging Technique give evidence of slowly-varying, long-living electric and/or magnetic structures generated by laser-plasma interaction

[Kar et al, New J. Phys. **9**, 502 (2007);
Liseikina et al, arXiv:physics/0702177]



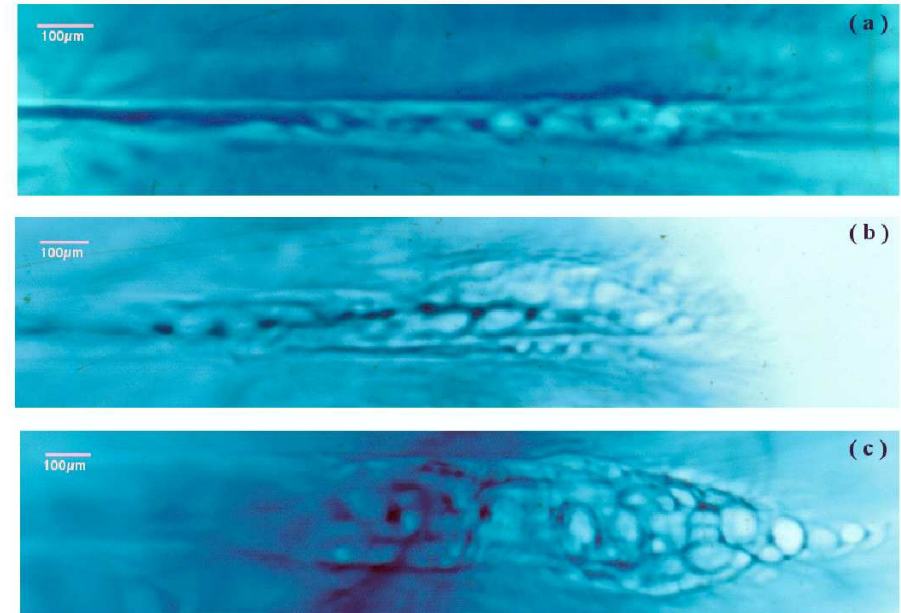
Challenge: make simulations with spatial and temporal scales as close as possible to the experiment



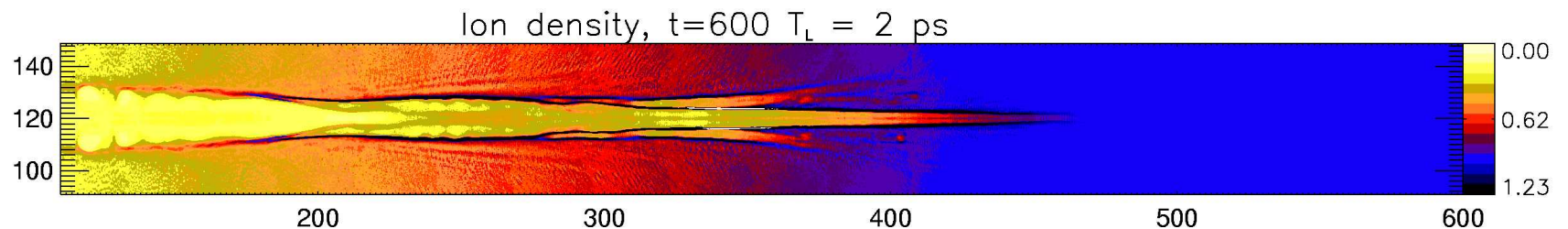
“Coherent” EM structures observed?

Experimental data from the Proton Imaging Technique give evidence of slowly-varying, long-living electric and/or magnetic structures generated by laser-plasma interaction

[Kar et al, New J. Phys. **9**, 502 (2007);
Liseikina et al, arXiv:physics/0702177]



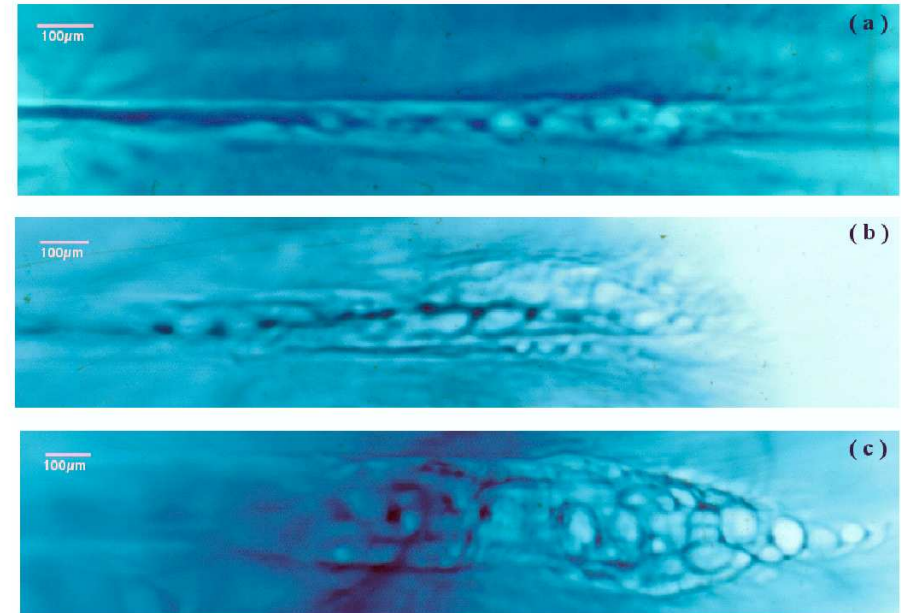
Challenge: make simulations with spatial and temporal scales as close as possible to the experiment



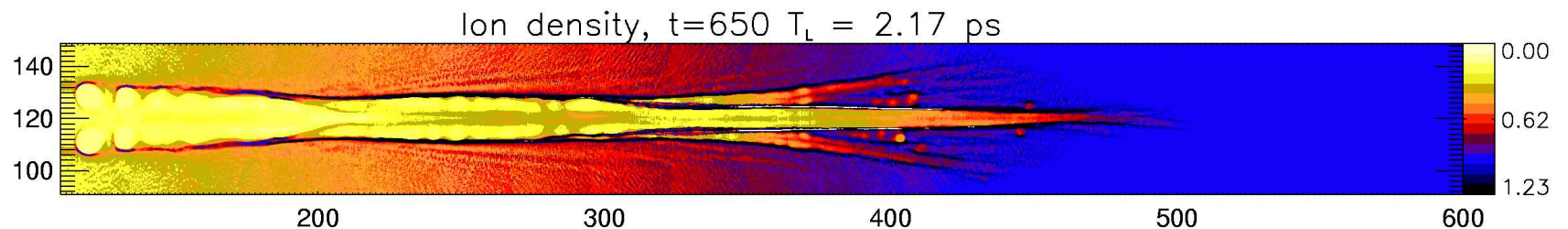
“Coherent” EM structures observed?

Experimental data from the Proton Imaging Technique give evidence of slowly-varying, long-living electric and/or magnetic structures generated by laser-plasma interaction

[Kar et al, New J. Phys. **9**, 502 (2007);
Liseikina et al, arXiv:physics/0702177]



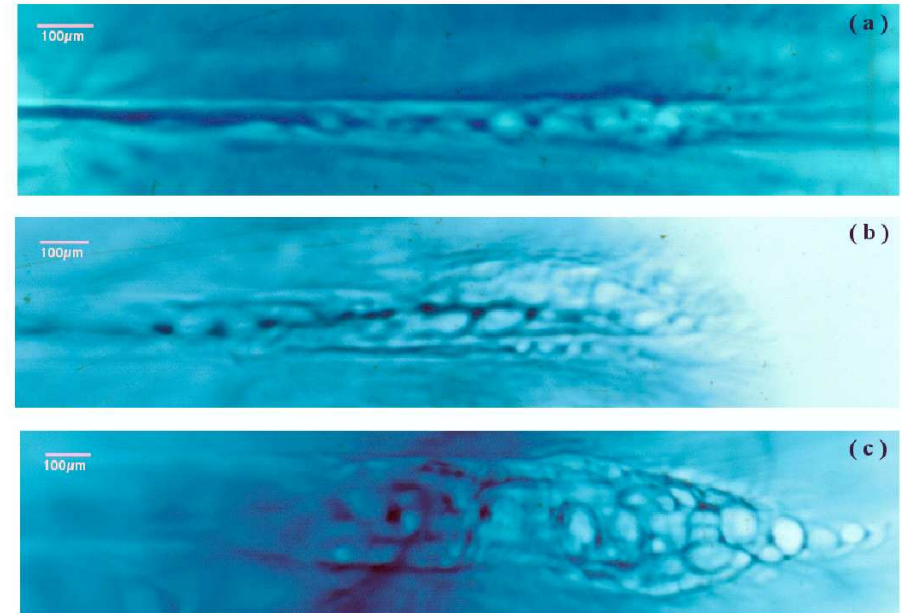
Challenge: make simulations with spatial and temporal scales as close as possible to the experiment



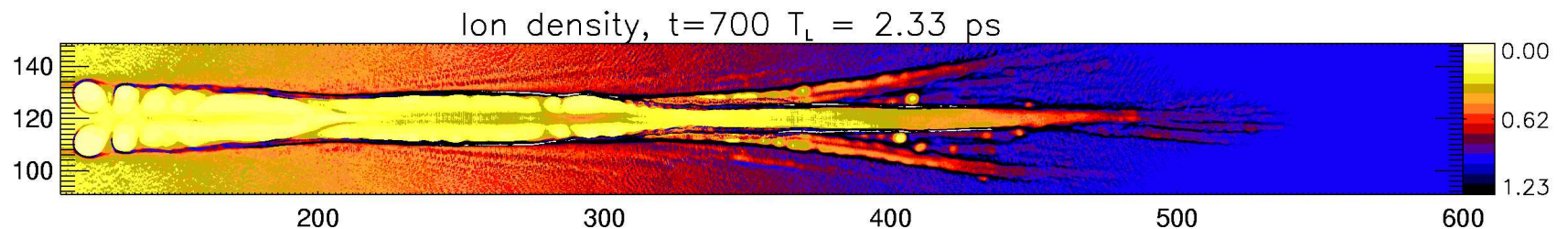
“Coherent” EM structures observed?

Experimental data from the Proton Imaging Technique give evidence of slowly-varying, long-living electric and/or magnetic structures generated by laser-plasma interaction

[Kar et al, New J. Phys. **9**, 502 (2007);
Liseikina et al, arXiv:physics/0702177]



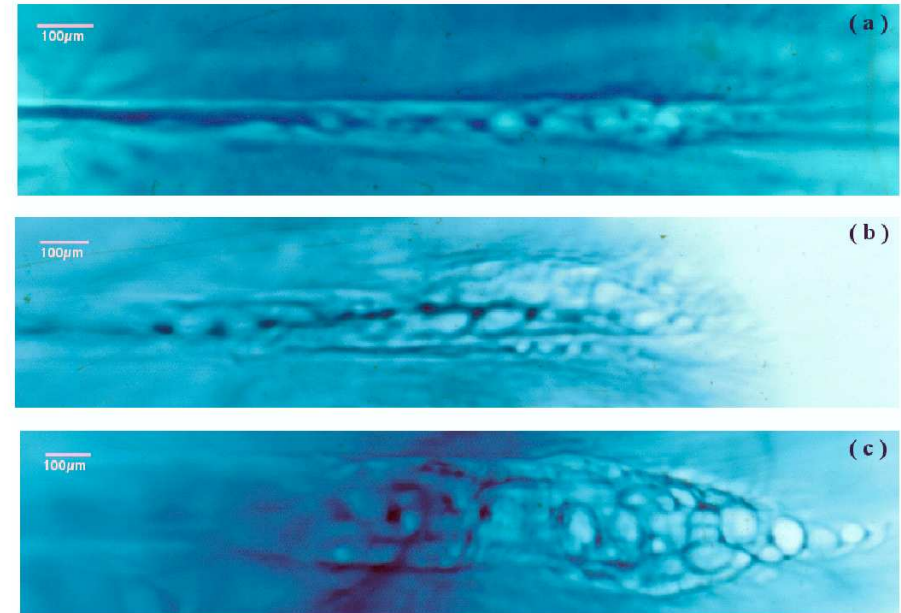
Challenge: make simulations with spatial and temporal scales as close as possible to the experiment



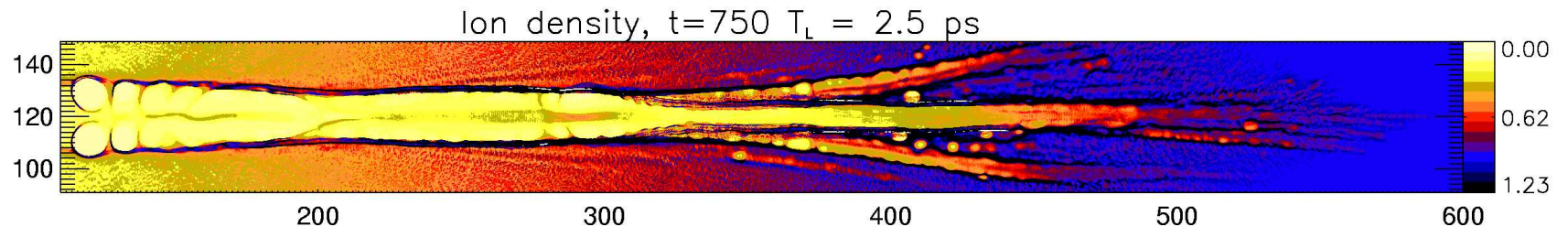
“Coherent” EM structures observed?

Experimental data from the Proton Imaging Technique give evidence of slowly-varying, long-living electric and/or magnetic structures generated by laser-plasma interaction

[Kar et al, New J. Phys. **9**, 502 (2007);
Liseikina et al, arXiv:physics/0702177]



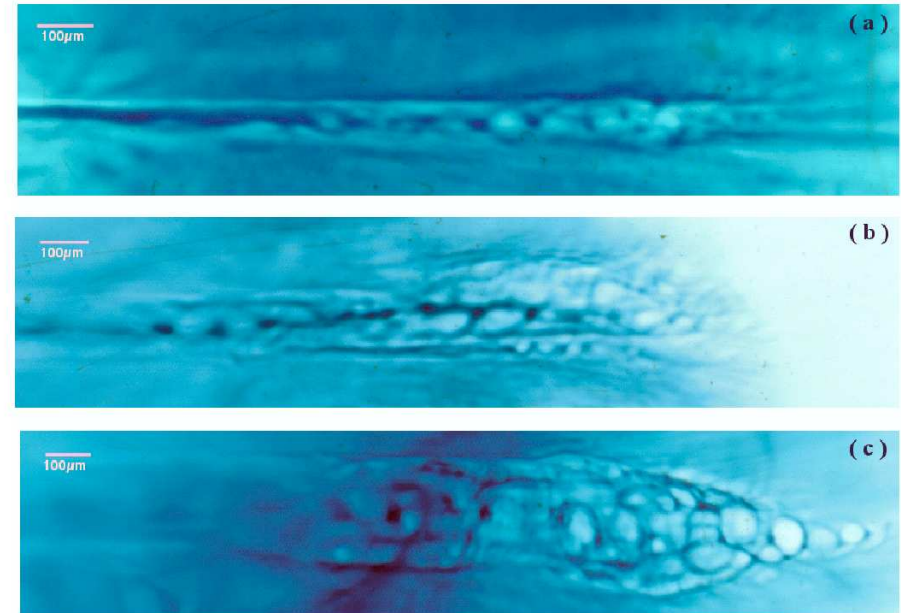
Challenge: make simulations with spatial and temporal scales as close as possible to the experiment



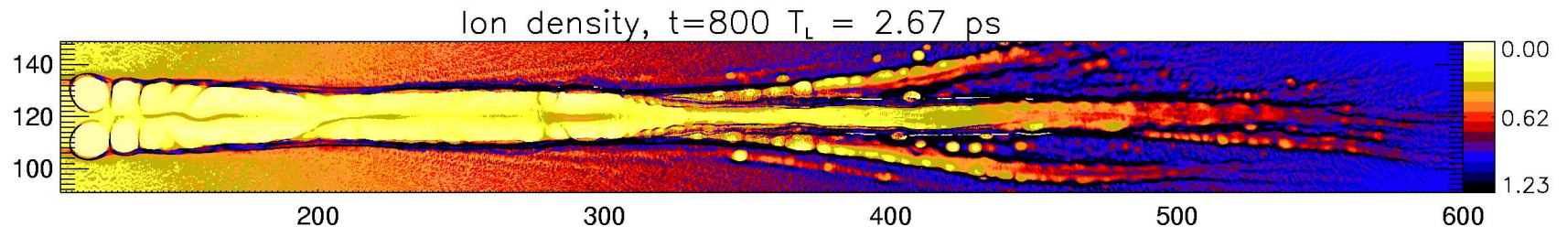
“Coherent” EM structures observed?

Experimental data from the Proton Imaging Technique give evidence of slowly-varying, long-living electric and/or magnetic structures generated by laser-plasma interaction

[Kar et al, New J. Phys. **9**, 502 (2007);
Liseikina et al, arXiv:physics/0702177]



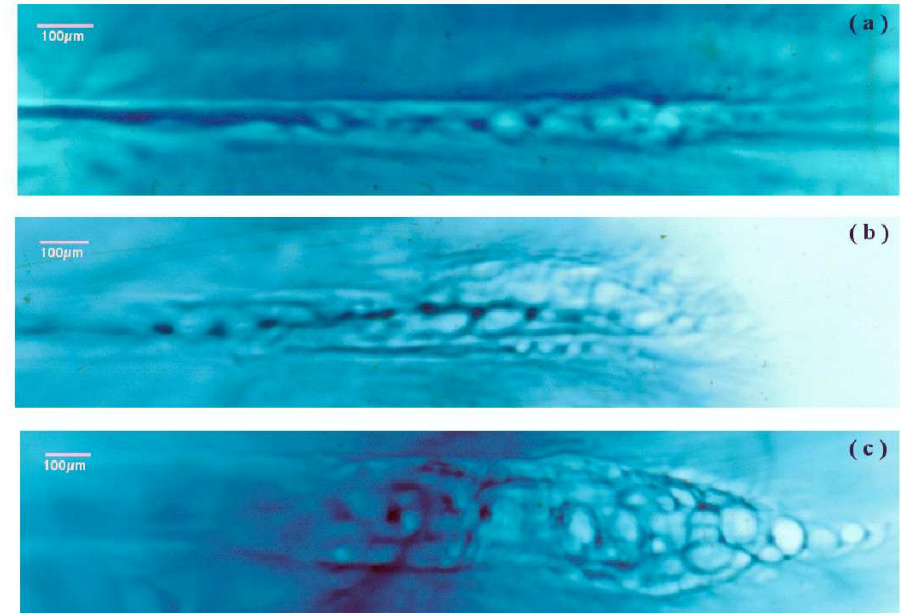
Challenge: make simulations with spatial and temporal scales as close as possible to the experiment



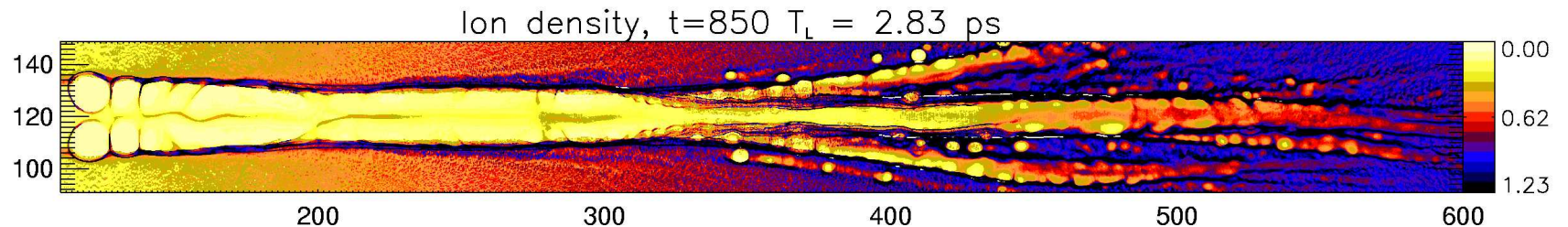
“Coherent” EM structures observed?

Experimental data from the Proton Imaging Technique give evidence of slowly-varying, long-living electric and/or magnetic structures generated by laser-plasma interaction

[Kar et al, New J. Phys. **9**, 502 (2007);
Liseikina et al, arXiv:physics/0702177]



Challenge: make simulations with spatial and temporal scales as close as possible to the experiment



Simulation set-up

Simulation set-up

Particle-in-Cell (PIC) simulations in 2D cartesian geometry

Simulation set-up

Particle-in-Cell (PIC) simulations in 2D cartesian geometry

Laser pulse intensity

$I = 10^{18} \div 10^{19} \text{ W/cm}^2$,
pulse duration $\tau_L = 1 \text{ ps}$
for $\lambda = 1 \mu\text{m}$.

Simulation set-up

Particle-in-Cell (PIC) simulations in 2D cartesian geometry

Laser pulse intensity

$I = 10^{18} \div 10^{19} \text{ W/cm}^2$,
pulse duration $\tau_L = 1 \text{ ps}$
for $\lambda = 1 \mu\text{m}$.

Box size $650\lambda \times 120\lambda$
= 6500×1200 gridpoints

$\sim 2 \times 10^8$ particles (16 per cell) ~ 13500 timesteps

~ 24 hours of CPU on ~ 50 processors

Simulation set-up

Particle-in-Cell (PIC) simulations in 2D cartesian geometry

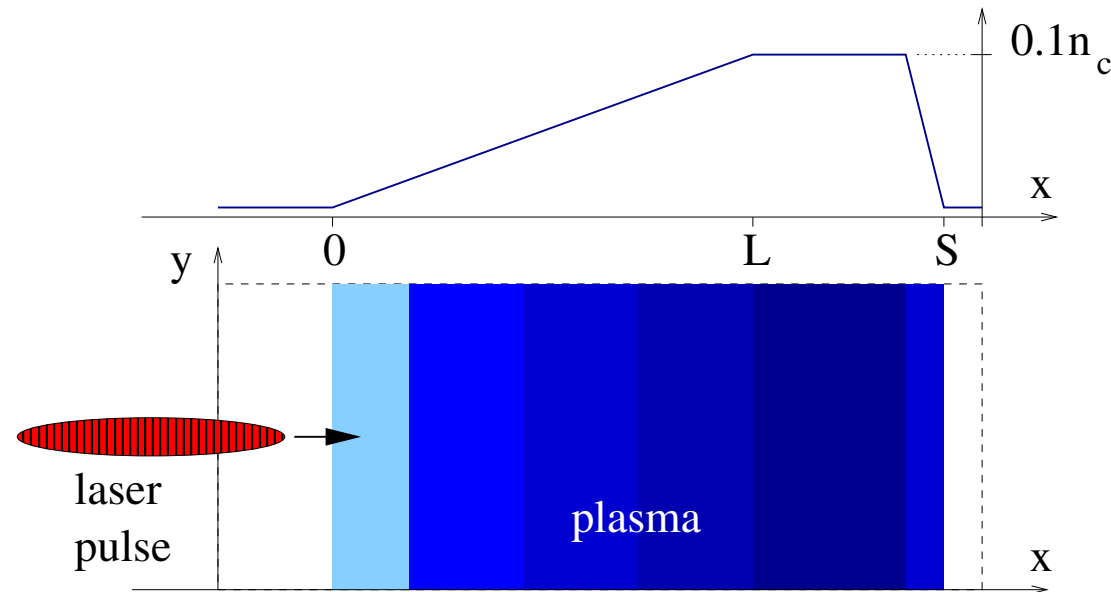
Laser pulse intensity

$I = 10^{18} \div 10^{19} \text{ W/cm}^2$,
pulse duration $\tau_L = 1 \text{ ps}$
for $\lambda = 1 \mu\text{m}$.

Box size $650\lambda \times 120\lambda$
 $= 6500 \times 1200 \text{ gridpoints}$

$\sim 2 \times 10^8$ particles (16 per cell) ~ 13500 timesteps

~ 24 hours of CPU on ~ 50 processors



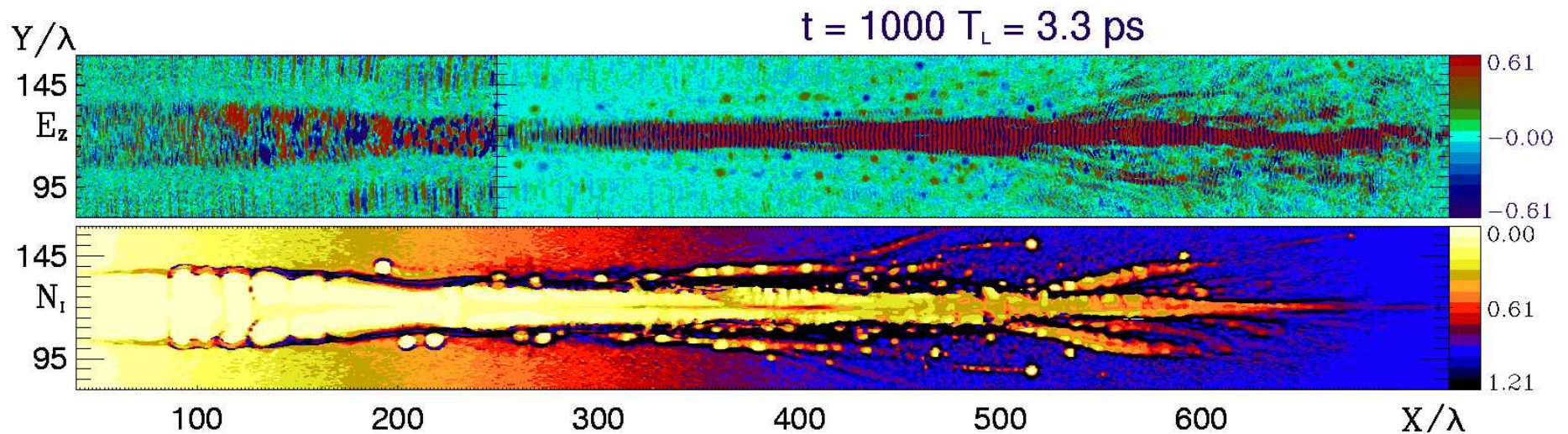
Slowly-varying EM structures

Slowly-varying EM structures

Generation of both isolated and pattern-organized field structures

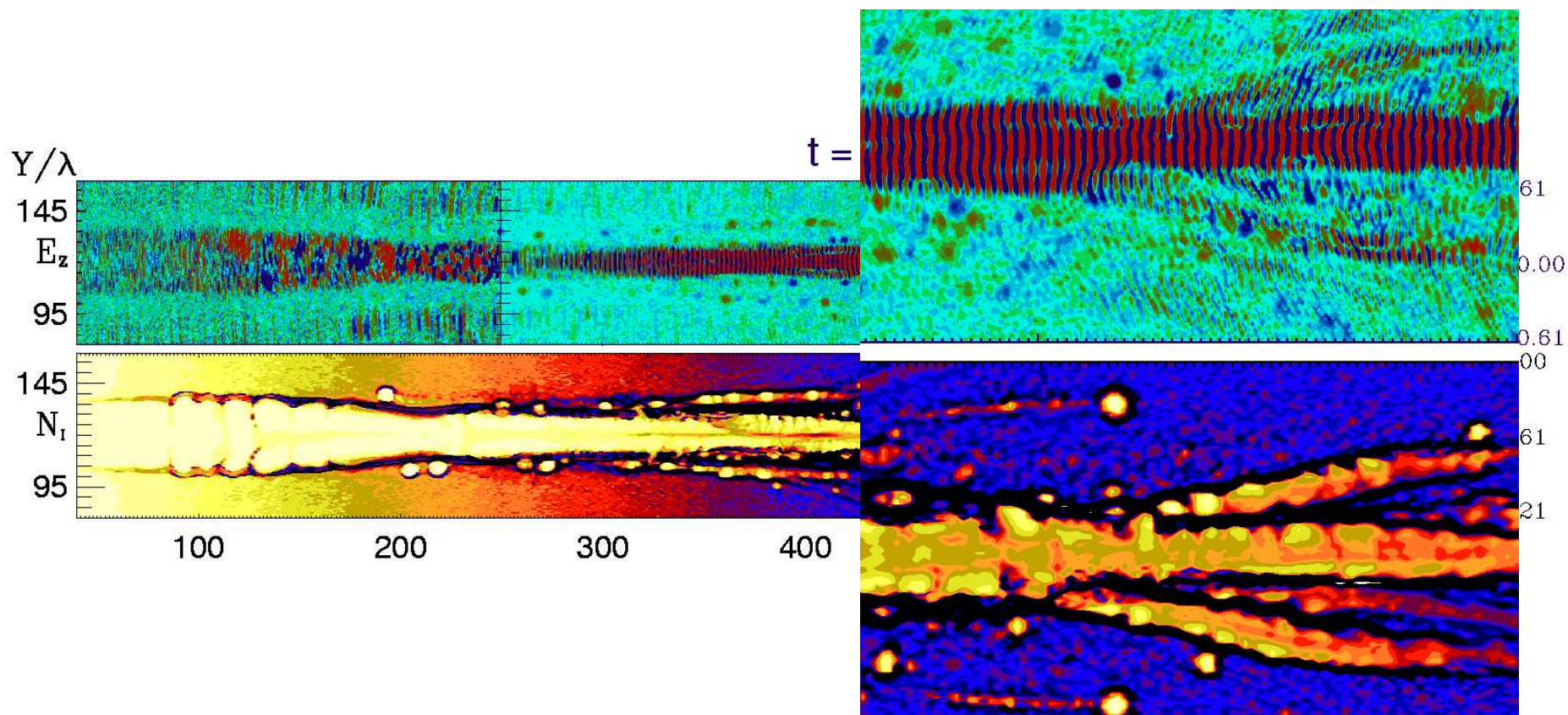
Slowly-varying EM structures

Generation of both isolated and pattern-organized field structures



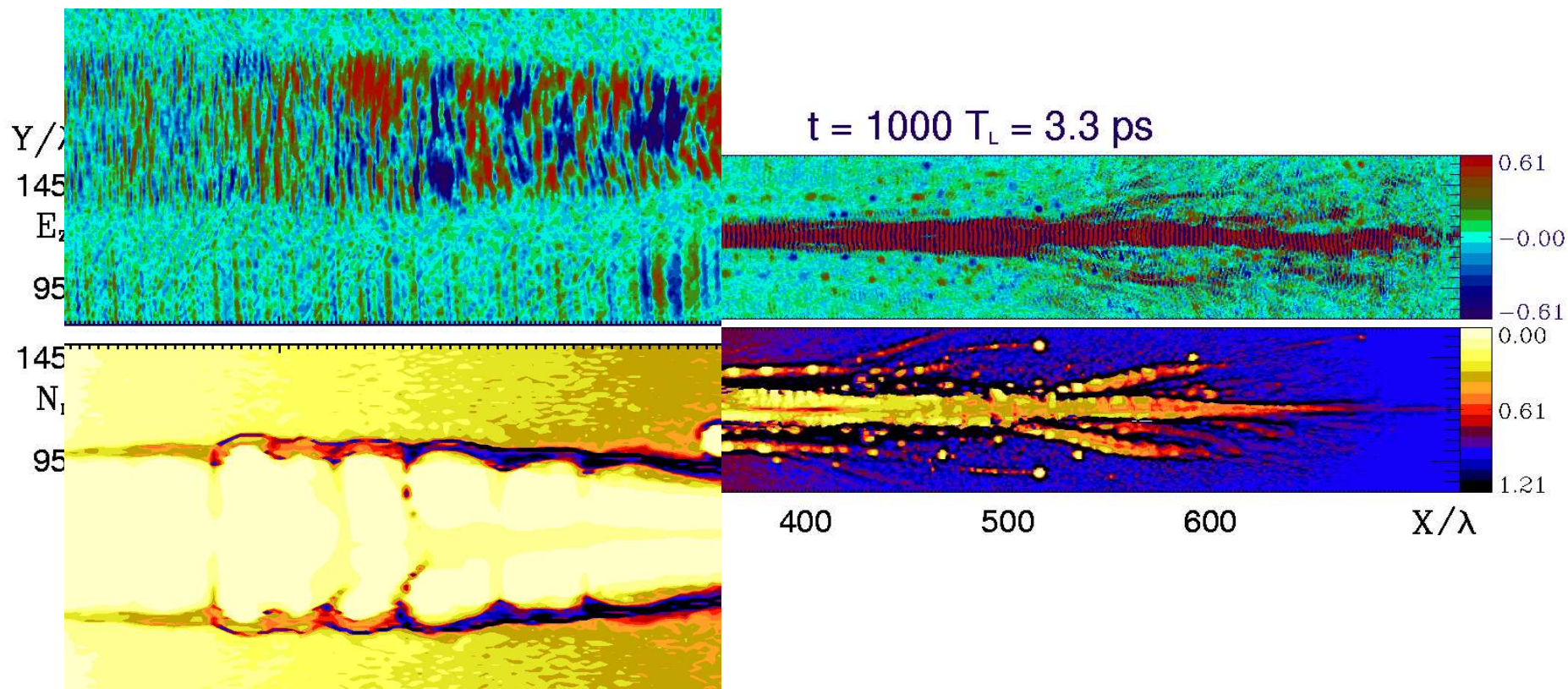
Slowly-varying EM structures

Both isolated “cavitons” or “post-solitons” and patterns inside density channels



Slowly-varying EM structures

Axially symmetrical pattern inside the main channel, in the low-density region



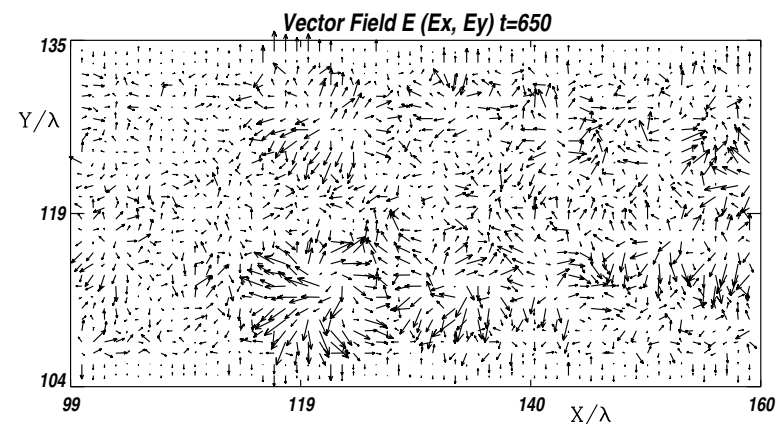
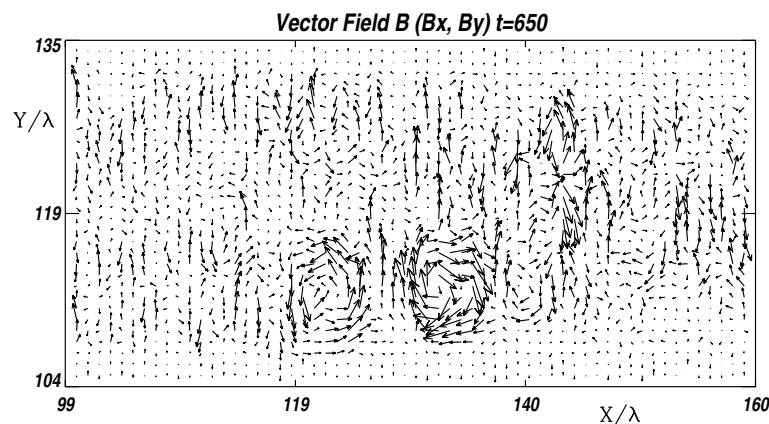
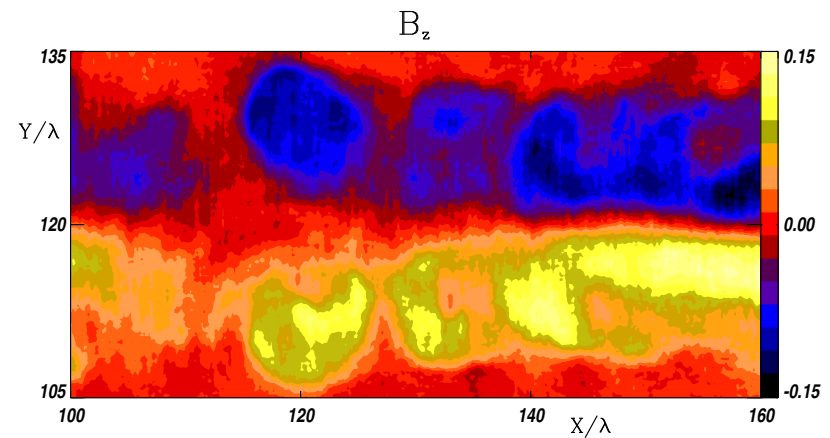
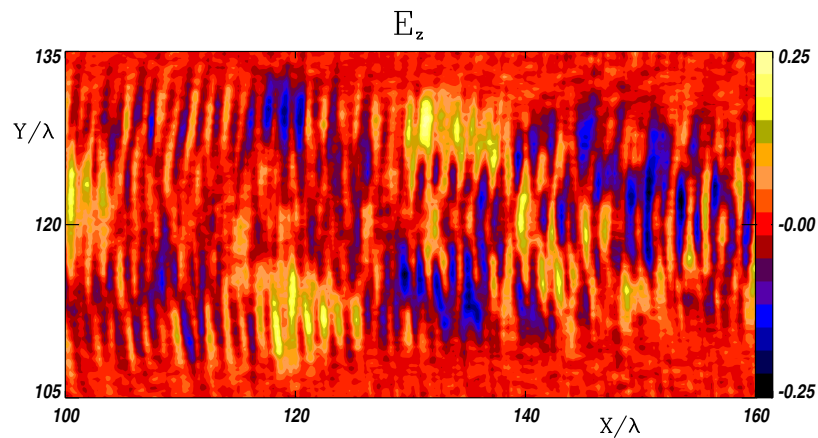
“Hybrid” electromagnetic structures

“Hybrid” electromagnetic structures

Structures from the pattern in the low-density region reveal a hybrid “vortex-caviton” nature with both **oscillating** and **quasi-static** components

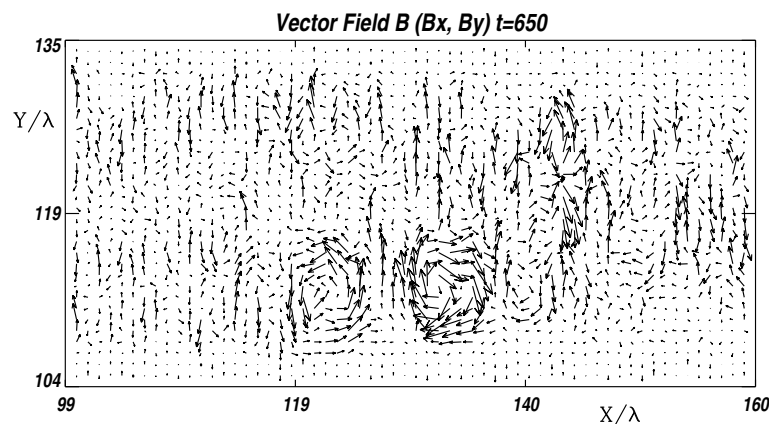
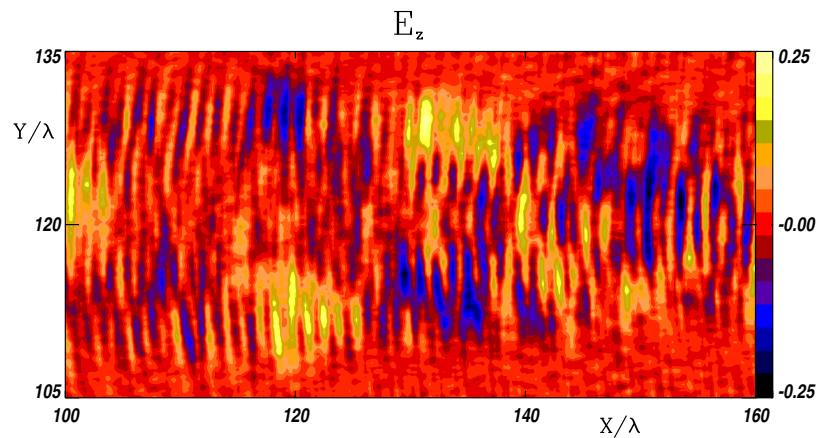
“Hybrid” electromagnetic structures

Structures from the pattern in the low-density region reveal a hybrid “vortex-caviton” nature with both **oscillating** and **quasi-static** components

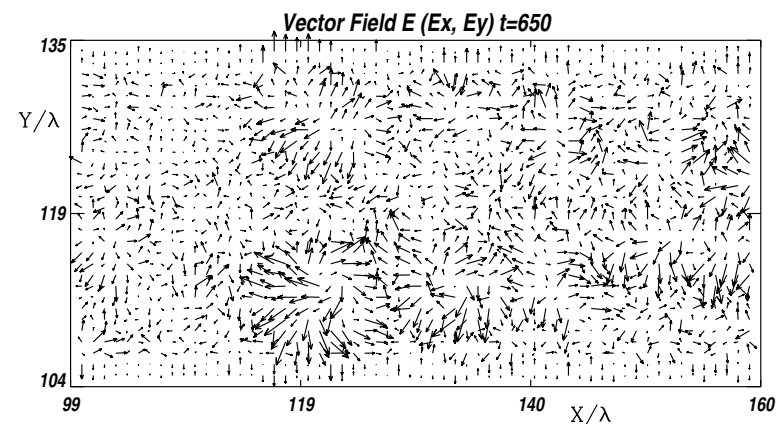
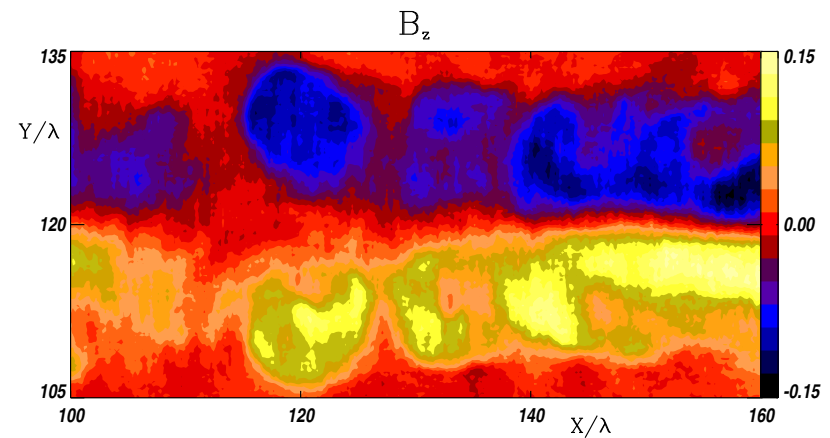


“Hybrid” electromagnetic structures

Structures from the pattern in the low-density region reveal a hybrid “vortex-caviton” nature with both **oscillating** and **quasi-static** components



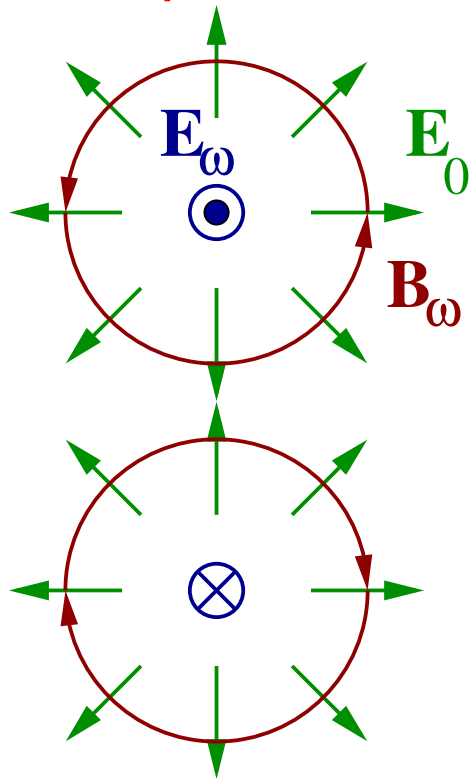
Oscillating (0.1ω)



Quasi-static

“Hybrid” electromagnetic structures

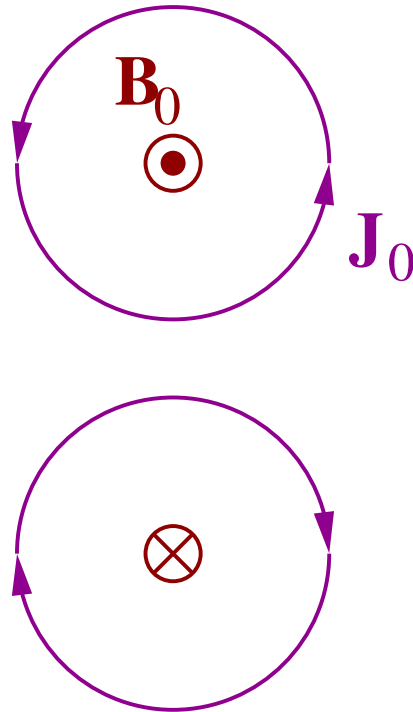
Structures from the pattern in the low-density region reveal a hybrid “vortex-caviton” nature with both **oscillating** and **quasi-static** components



Antisymmetric “soliton” fields:
oscillating E_z , B_x and B_y and
electrostatic E_x , E_y

“Hybrid” electromagnetic structures

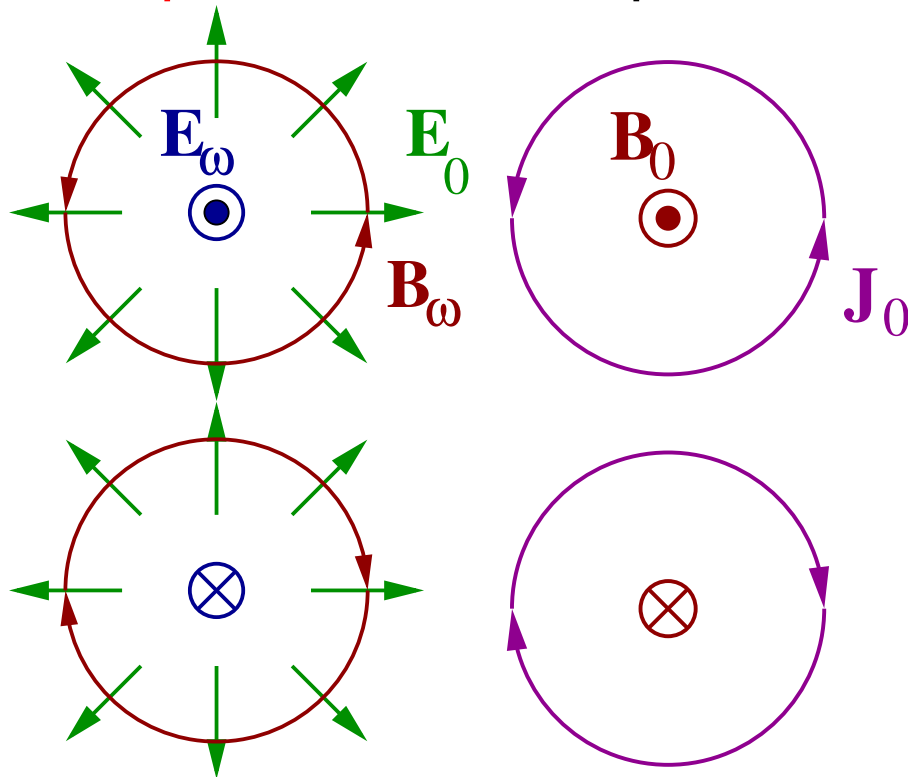
Structures from the pattern in the low-density region reveal a hybrid “vortex-caviton” nature with both **oscillating** and **quasi-static** components



Antisymmetric “vortex” fields:
static B_z , J_x and J_y

“Hybrid” electromagnetic structures

Structures from the pattern in the low-density region reveal a hybrid “vortex-caviton” nature with both **oscillating** and **quasi-static** components

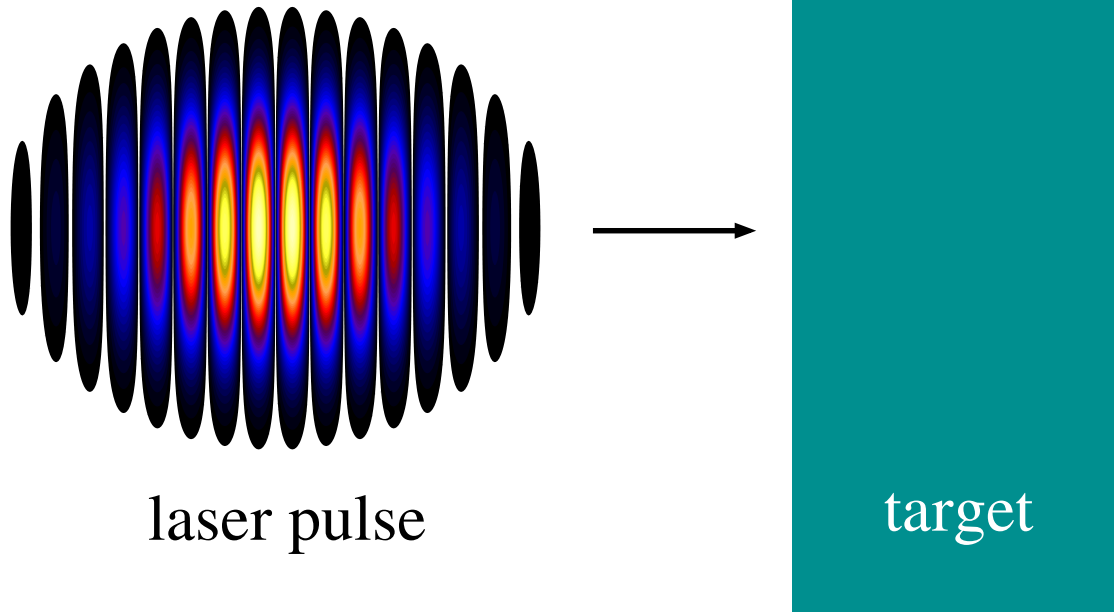


We may expect “toroidal” structures in 3D – related simulations are in progress (3200 × 320 × 320 grid, 8 points per λ , $\sim 5 \times 10^9$ particles – 8 per cell, 400 PEs, ~ 360 GBytes load)

Radiation Pressure Acceleration

Radiation Pressure Acceleration

Goal: accelerate plasma ions to high energies using the radiation pressure of the laser pulse



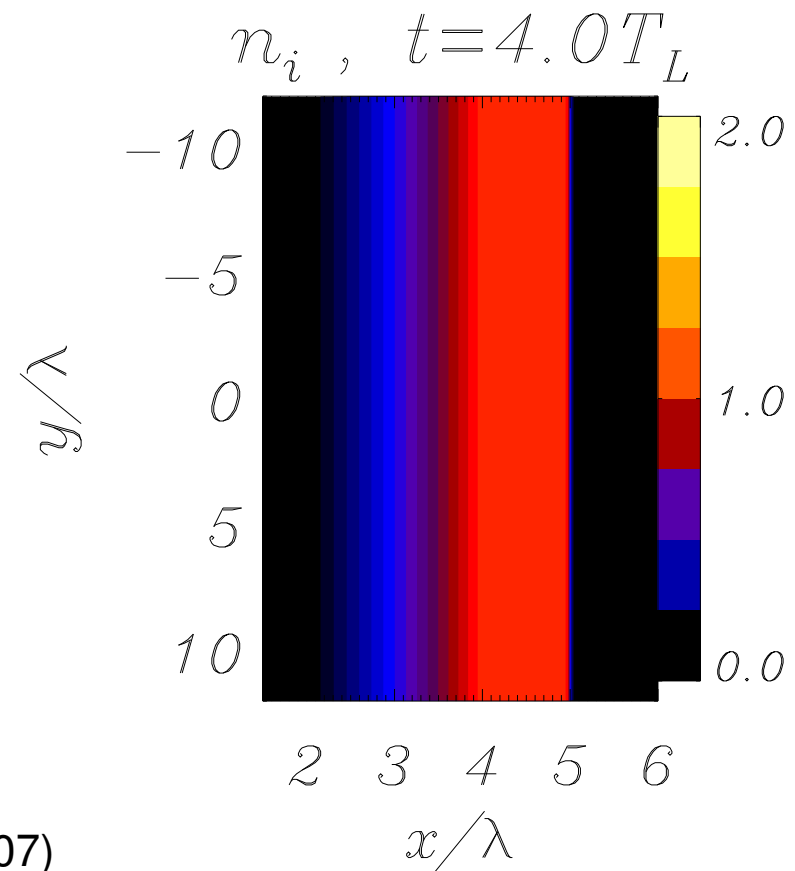
Radiation Pressure Acceleration

Goal: accelerate plasma ions to high energies using the radiation pressure of the laser pulse

- Relevant to foreseeable applications (e.g. medical hadrontherapy)
- May be the dominant acceleration mechanism in the ELI experiment (www.eli-laser.eu)
- Use of **Circularly Polarized** pulses optimise RPA

Macchi et al, Phys. Rev. Lett **94**, 165003 (2005);

Liseikina and Macchi, Appl. Phys. Lett. **91**, 171502 (2007)



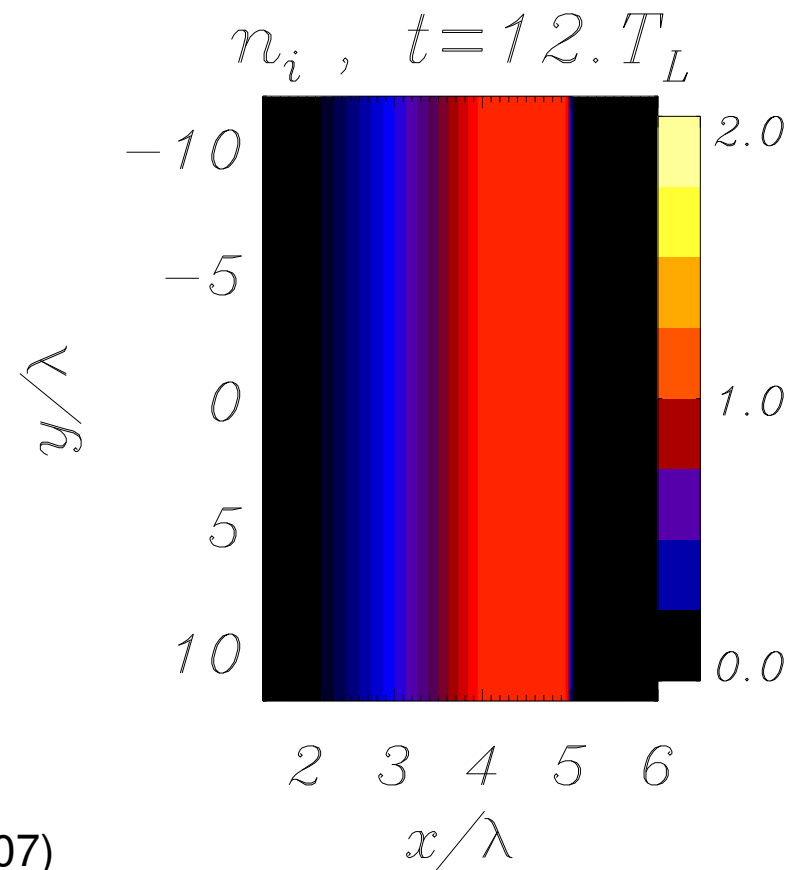
Radiation Pressure Acceleration

Goal: accelerate plasma ions to high energies using the radiation pressure of the laser pulse

- Relevant to foreseeable applications (e.g. medical hadrontherapy)
- May be the dominant acceleration mechanism in the ELI experiment (www.eli-laser.eu)
- Use of **Circularly Polarized** pulses optimise RPA

Macchi et al, Phys. Rev. Lett **94**, 165003 (2005);

Liseikina and Macchi, Appl. Phys. Lett. **91**, 171502 (2007)



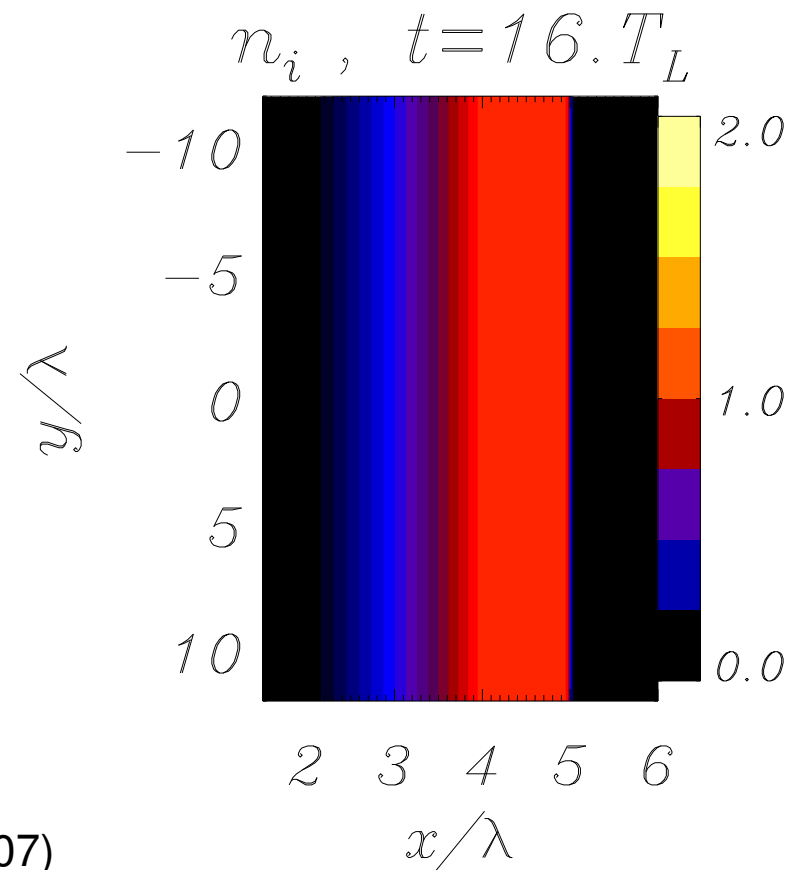
Radiation Pressure Acceleration

Goal: accelerate plasma ions to high energies using the radiation pressure of the laser pulse

- Relevant to foreseeable applications (e.g. medical hadrontherapy)
- May be the dominant acceleration mechanism in the ELI experiment (www.eli-laser.eu)
- Use of **Circularly Polarized** pulses optimise RPA

Macchi et al, Phys. Rev. Lett **94**, 165003 (2005);

Liseikina and Macchi, Appl. Phys. Lett. **91**, 171502 (2007)



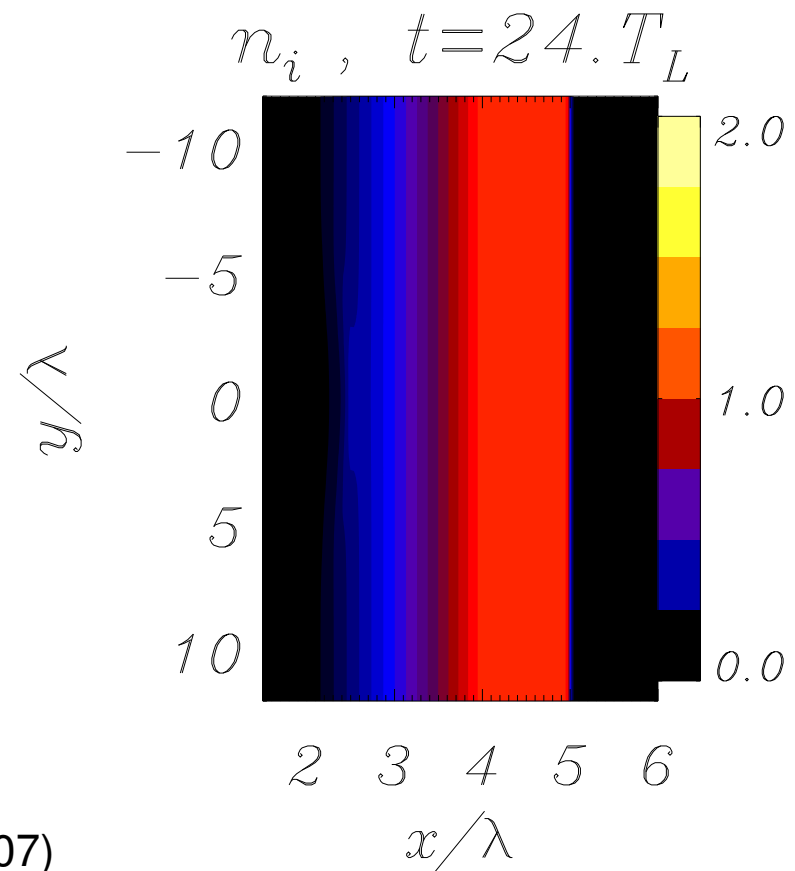
Radiation Pressure Acceleration

Goal: accelerate plasma ions to high energies using the radiation pressure of the laser pulse

- Relevant to foreseeable applications (e.g. medical hadrontherapy)
- May be the dominant acceleration mechanism in the ELI experiment (www.eli-laser.eu)
- Use of **Circularly Polarized** pulses optimise RPA

Macchi et al, Phys. Rev. Lett **94**, 165003 (2005);

Liseikina and Macchi, Appl. Phys. Lett. **91**, 171502 (2007)



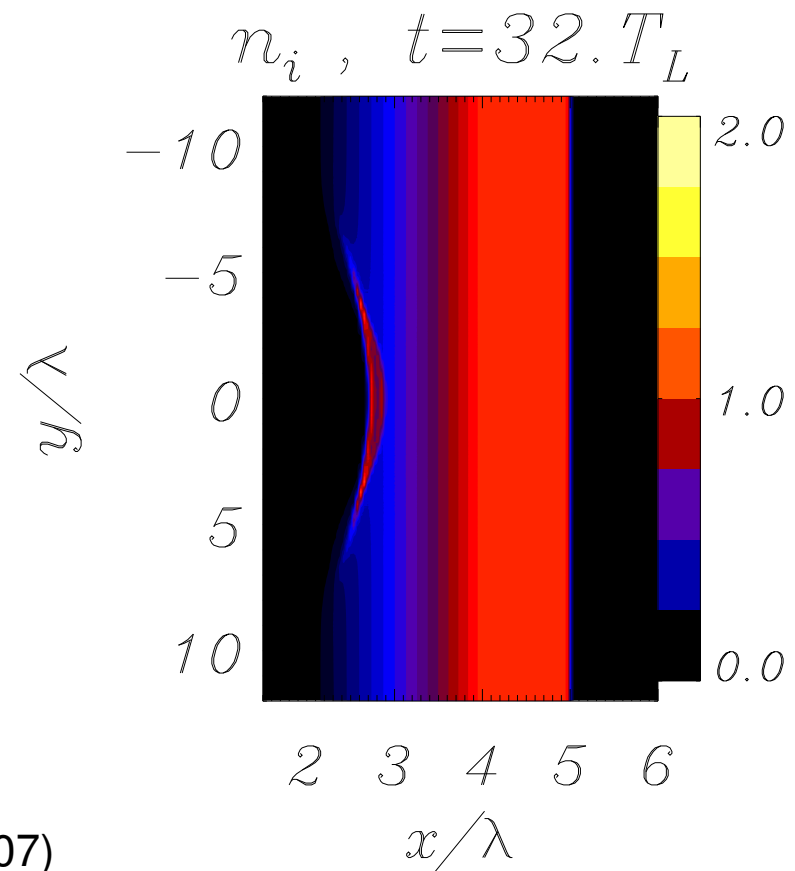
Radiation Pressure Acceleration

Goal: accelerate plasma ions to high energies using the radiation pressure of the laser pulse

- Relevant to foreseeable applications (e.g. medical hadrontherapy)
- May be the dominant acceleration mechanism in the ELI experiment (www.eli-laser.eu)
- Use of **Circularly Polarized** pulses optimise RPA

Macchi et al, Phys. Rev. Lett **94**, 165003 (2005);

Liseikina and Macchi, Appl. Phys. Lett. **91**, 171502 (2007)



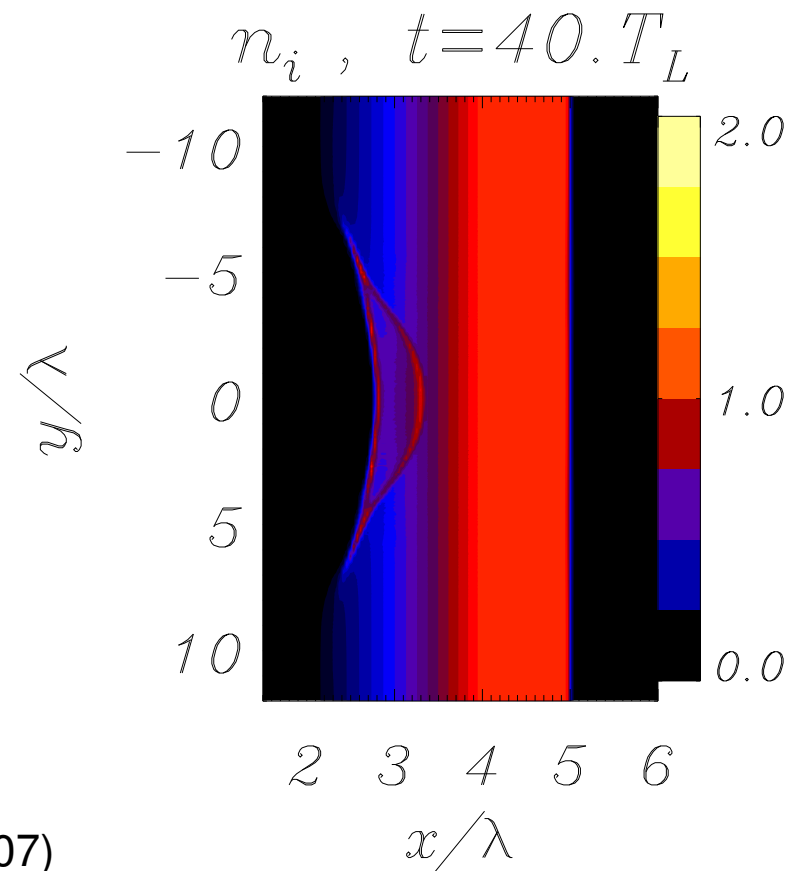
Radiation Pressure Acceleration

Goal: accelerate plasma ions to high energies using the radiation pressure of the laser pulse

- Relevant to foreseeable applications (e.g. medical hadrontherapy)
- May be the dominant acceleration mechanism in the ELI experiment (www.eli-laser.eu)
- Use of **Circularly Polarized** pulses optimise RPA

Macchi et al, Phys. Rev. Lett **94**, 165003 (2005);

Liseikina and Macchi, Appl. Phys. Lett. **91**, 171502 (2007)



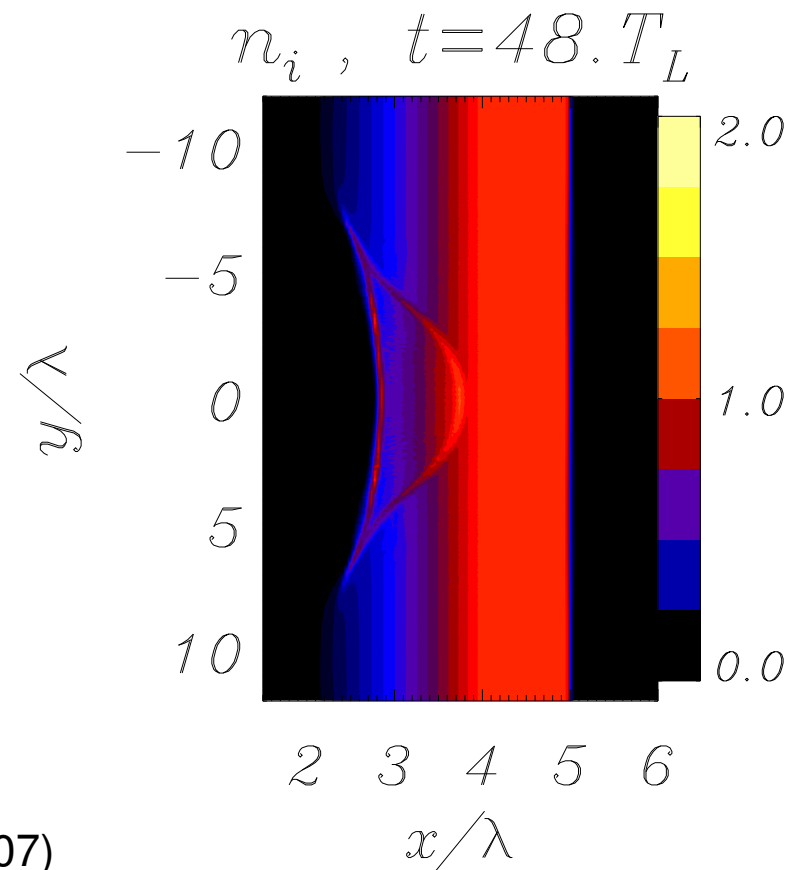
Radiation Pressure Acceleration

Goal: accelerate plasma ions to high energies using the radiation pressure of the laser pulse

- Relevant to foreseeable applications (e.g. medical hadrontherapy)
- May be the dominant acceleration mechanism in the ELI experiment (www.eli-laser.eu)
- Use of **Circularly Polarized** pulses optimise RPA

Macchi et al, Phys. Rev. Lett **94**, 165003 (2005);

Liseikina and Macchi, Appl. Phys. Lett. **91**, 171502 (2007)



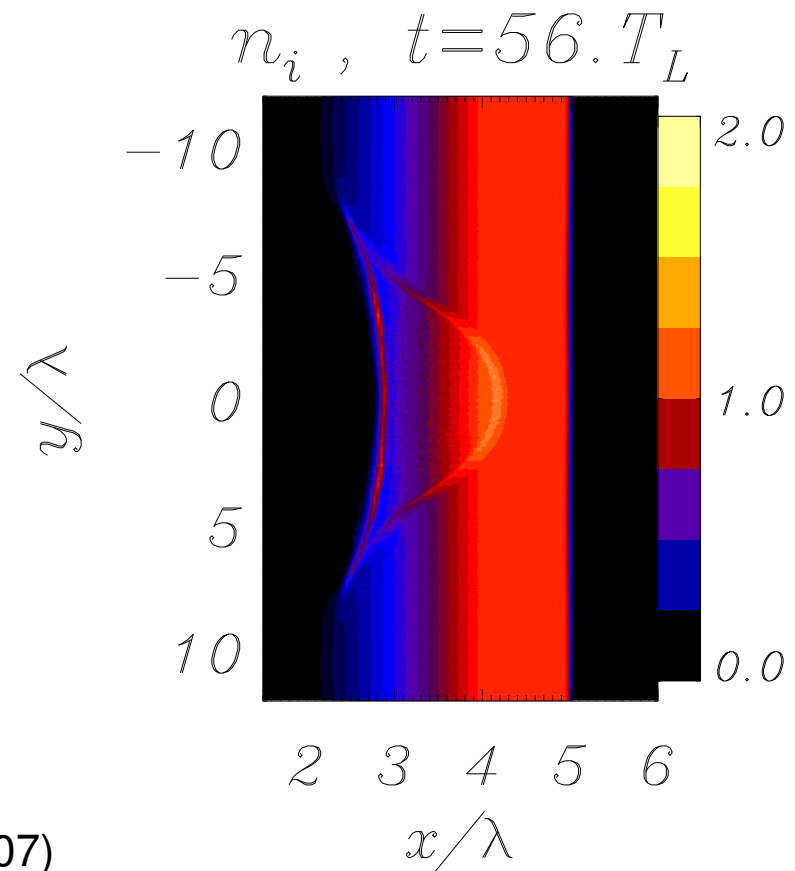
Radiation Pressure Acceleration

Goal: accelerate plasma ions to high energies using the radiation pressure of the laser pulse

- Relevant to foreseeable applications (e.g. medical hadrontherapy)
- May be the dominant acceleration mechanism in the ELI experiment (www.eli-laser.eu)
- Use of **Circularly Polarized** pulses optimise RPA

Macchi et al, Phys. Rev. Lett **94**, 165003 (2005);

Liseikina and Macchi, Appl. Phys. Lett. **91**, 171502 (2007)



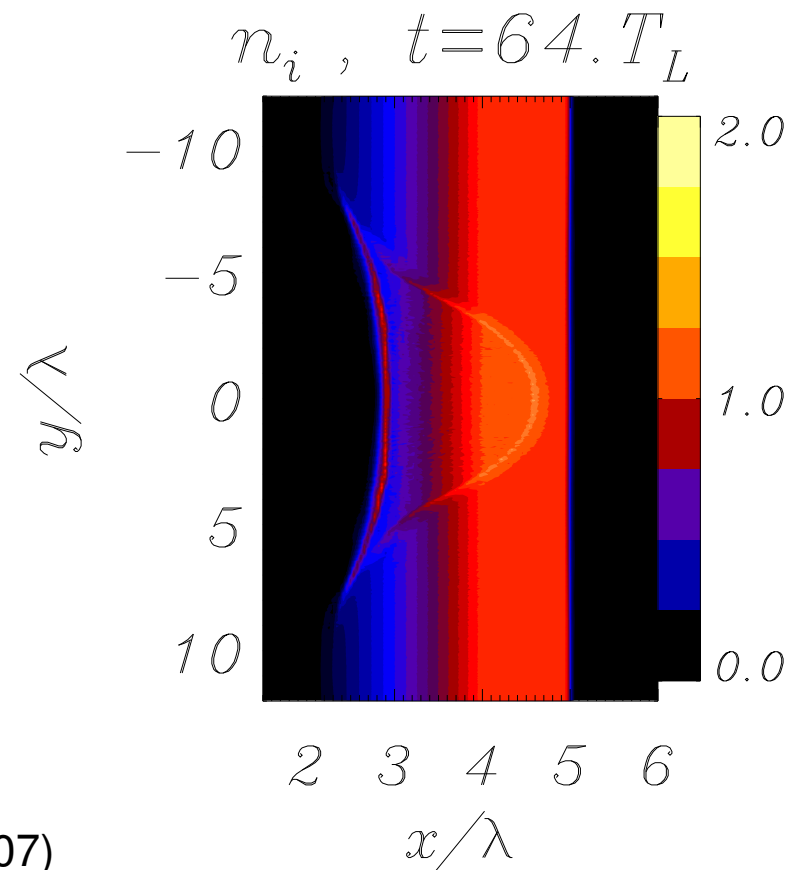
Radiation Pressure Acceleration

Goal: accelerate plasma ions to high energies using the radiation pressure of the laser pulse

- Relevant to foreseeable applications (e.g. medical hadrontherapy)
- May be the dominant acceleration mechanism in the ELI experiment (www.eli-laser.eu)
- Use of **Circularly Polarized** pulses optimise RPA

Macchi et al, Phys. Rev. Lett **94**, 165003 (2005);

Liseikina and Macchi, Appl. Phys. Lett. **91**, 171502 (2007)



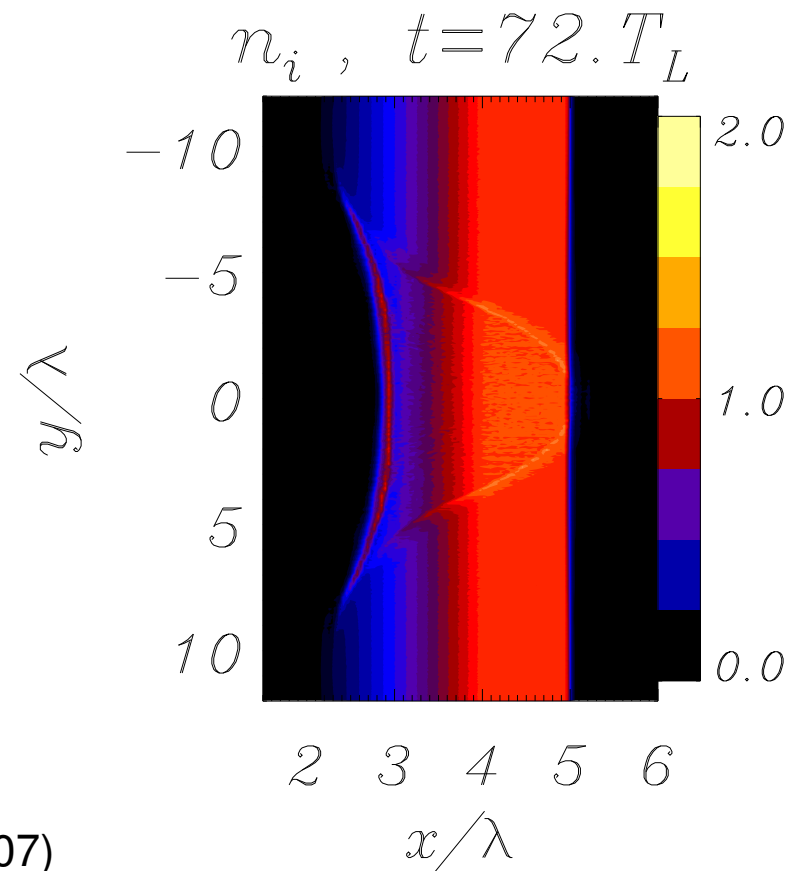
Radiation Pressure Acceleration

Goal: accelerate plasma ions to high energies using the radiation pressure of the laser pulse

- Relevant to foreseeable applications (e.g. medical hadrontherapy)
- May be the dominant acceleration mechanism in the ELI experiment (www.eli-laser.eu)
- Use of **Circularly Polarized** pulses optimise RPA

Macchi et al, Phys. Rev. Lett **94**, 165003 (2005);

Liseikina and Macchi, Appl. Phys. Lett. **91**, 171502 (2007)



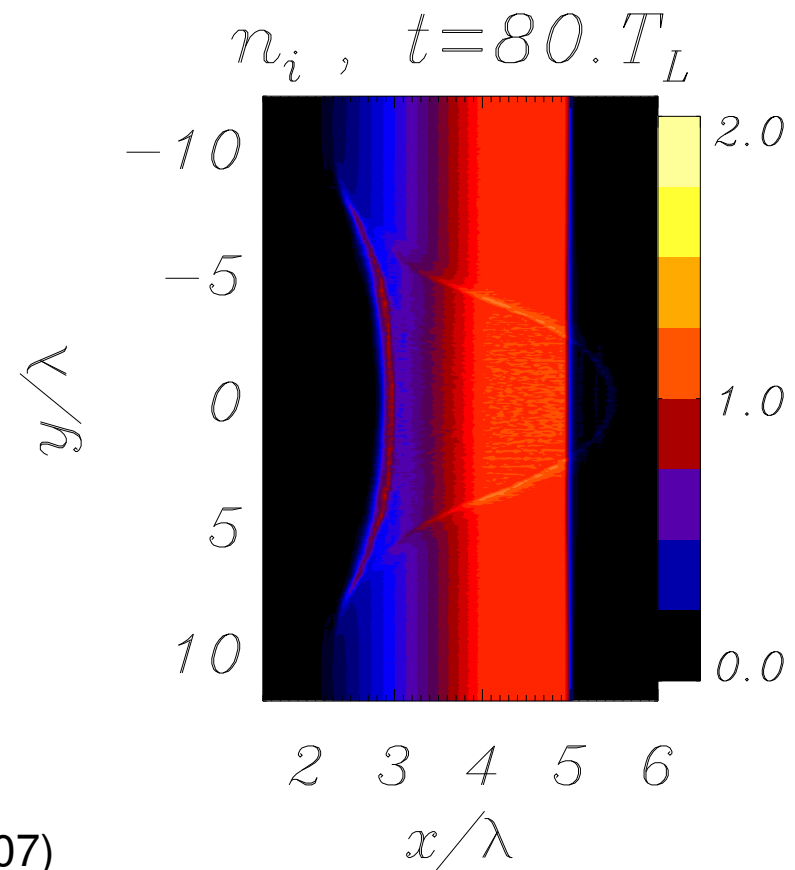
Radiation Pressure Acceleration

Goal: accelerate plasma ions to high energies using the radiation pressure of the laser pulse

- Relevant to foreseeable applications (e.g. medical hadrontherapy)
- May be the dominant acceleration mechanism in the ELI experiment (www.eli-laser.eu)
- Use of **Circularly Polarized** pulses optimise RPA

Macchi et al, Phys. Rev. Lett **94**, 165003 (2005);

Liseikina and Macchi, Appl. Phys. Lett. **91**, 171502 (2007)



3D issues in CP-RPA

3D issues in CP-RPA

- 3D simulations would generally be required for “physical realism”

3D issues in CP-RPA

- 3D simulations would generally be required for “physical realism”
- however, available computational resources limits 3D to “easy” parameters (low density, thin targets, short pulses, . . .)

3D issues in CP-RPA

- 3D simulations would generally be required for “physical realism”
- however, available computational resources limits 3D to “easy” parameters (low density, thin targets, short pulses, . . .)
- a CP pulse carries electromagnetic **angular momentum**: its conservation gives an additional constraint in 3D

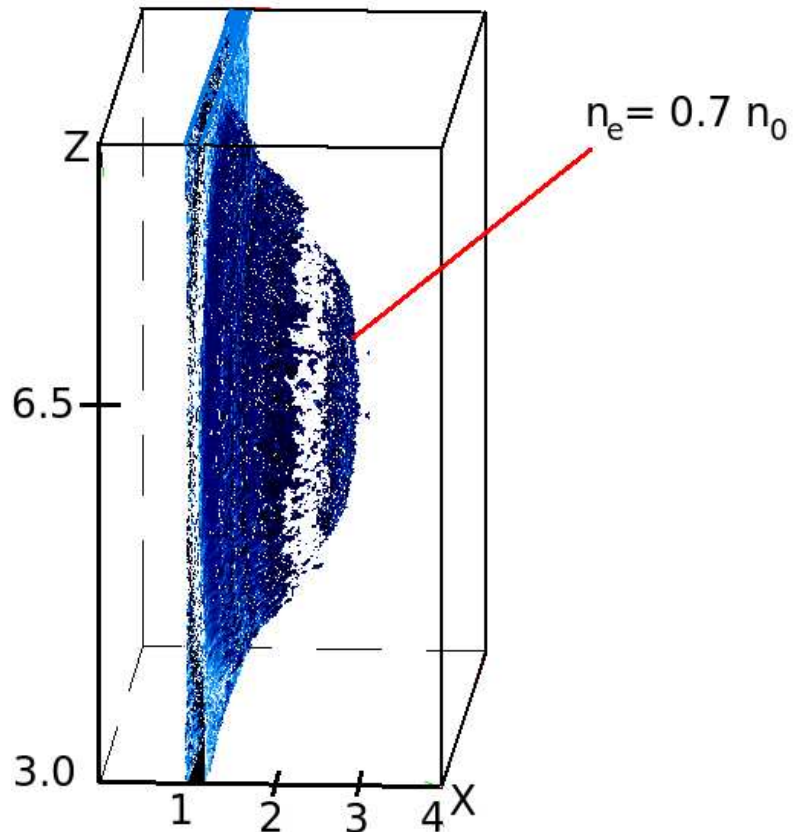
3D issues in CP-RPA

- 3D simulations would generally be required for “physical realism”
- however, available computational resources limits 3D to “easy” parameters (low density, thin targets, short pulses, . . .)
- a CP pulse carries electromagnetic **angular momentum**: its conservation gives an additional constraint in 3D
- theory shows that **absorption** of **angular momentum** does not occur for **adiabatic** acceleration of ions, thus it provides a diagnostic of the **non-adiabatic** or **dissipative** nature of energy transfer to ions (of possible interest for a **collisionless** system)

3D simulations of CP-RPA

plasma: $0.3\mu\text{m}$ slab with $n_e = 16n_c = 1.8 \times 10^{22} \text{ cm}^{-3}$

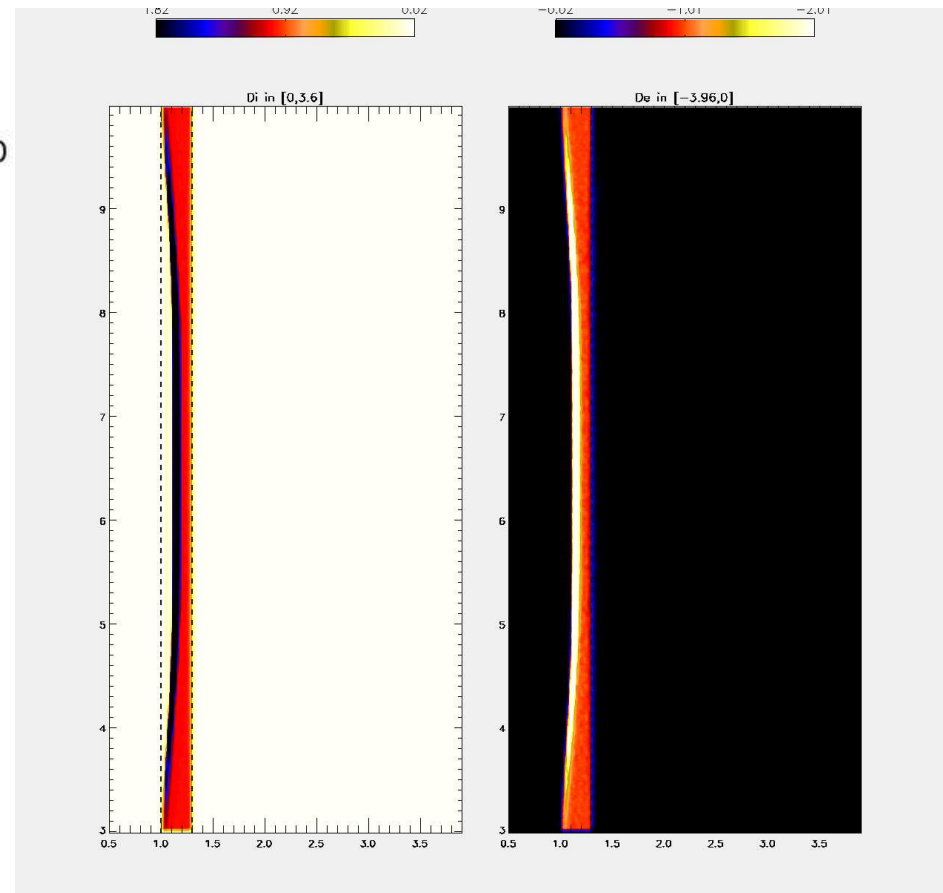
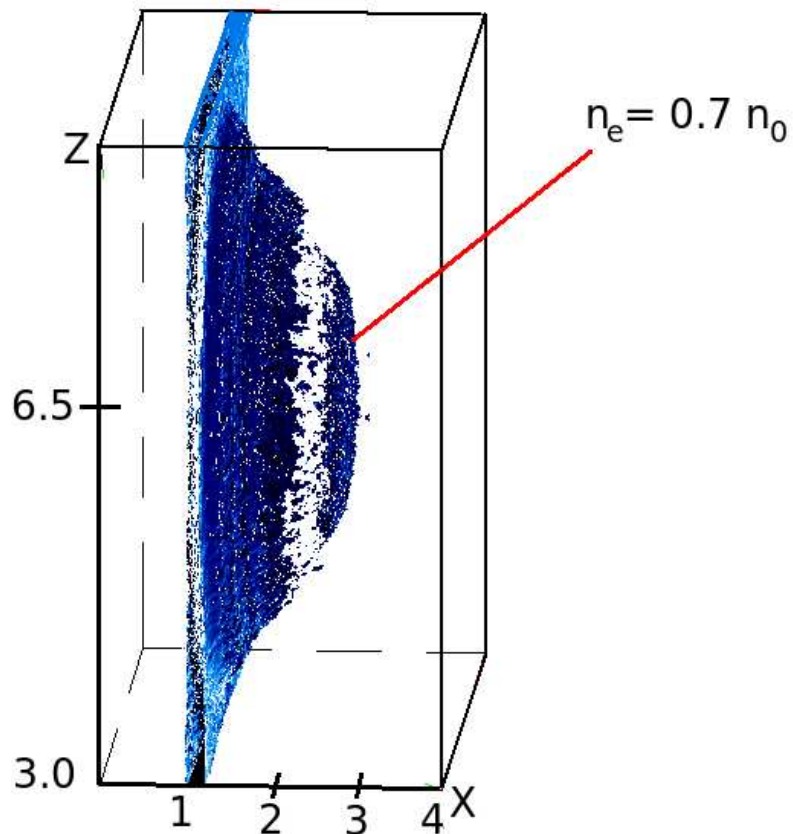
pulse: $I = 3.4 \times 10^{19} \text{ W/cm}^2$, $6\mu\text{m}$ focal diameter, 50 fs duration.



3D simulations of CP-RPA

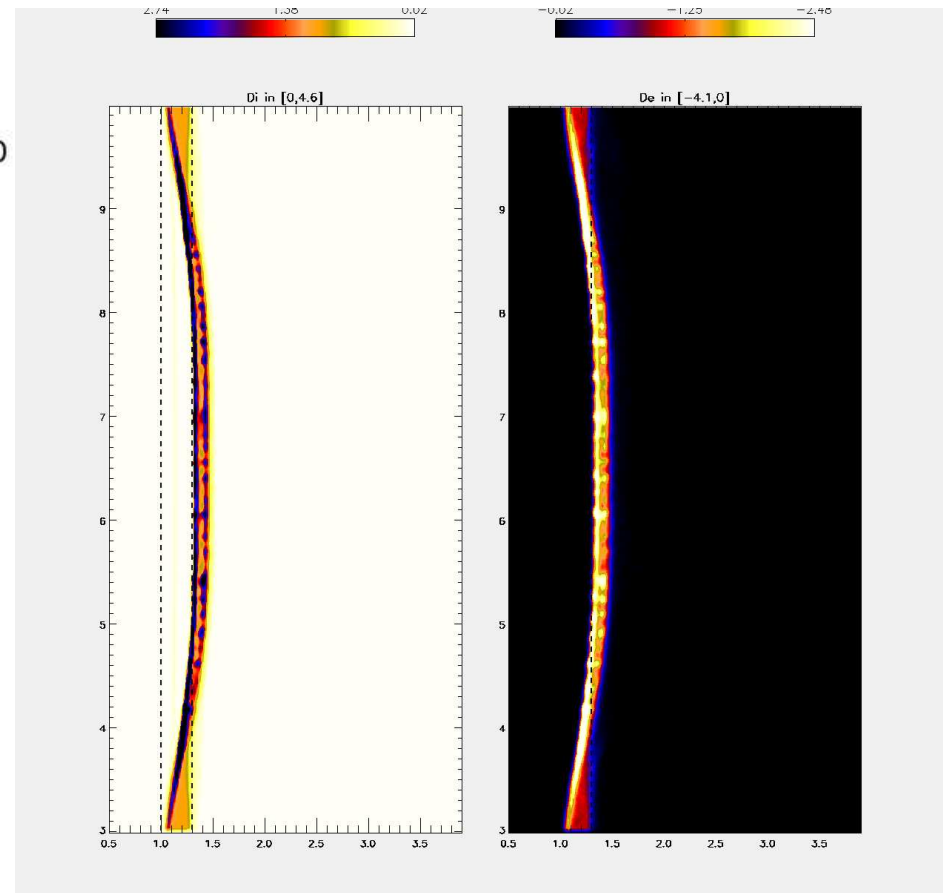
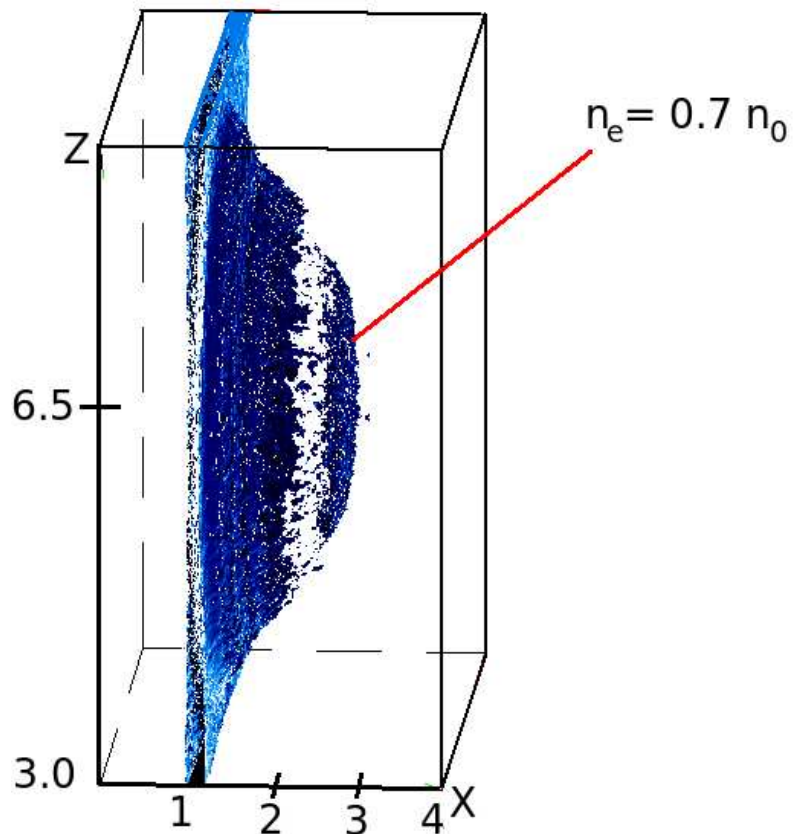
182 PEs, $320 \times 1050 \times 1050$ grid, 80 points per λ
 $\sim 1.5 \times 10^9$ particles (27 per cell), 360 GBytes load

Ion density (thin foil target)



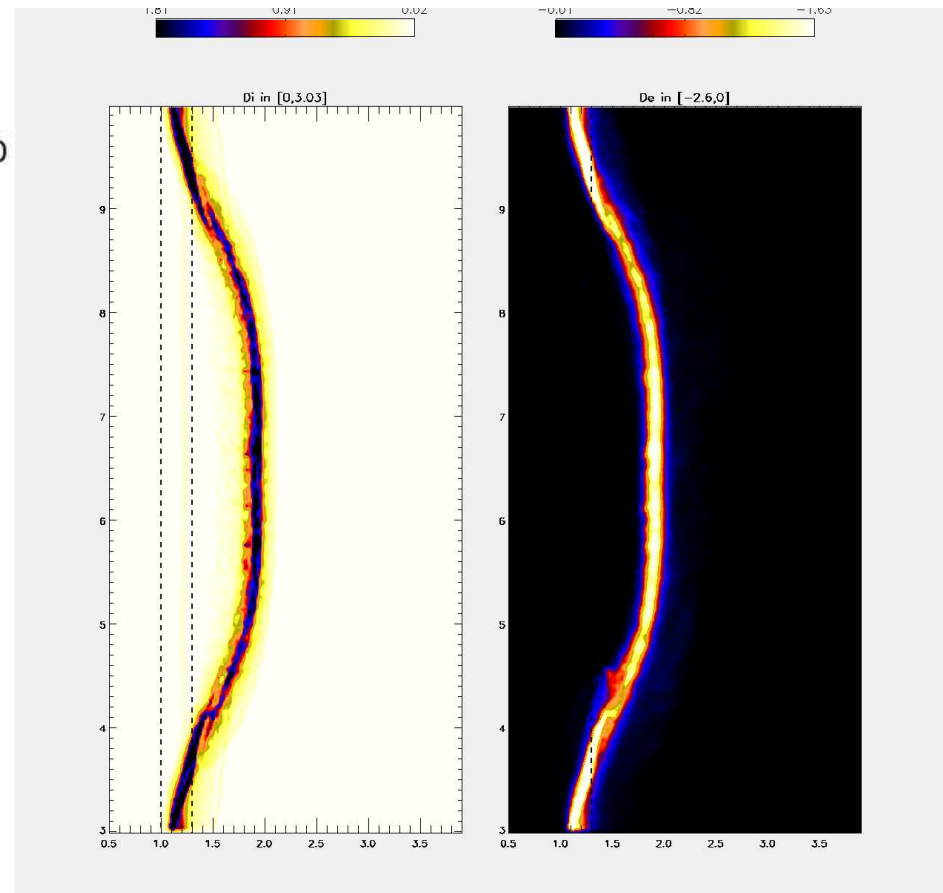
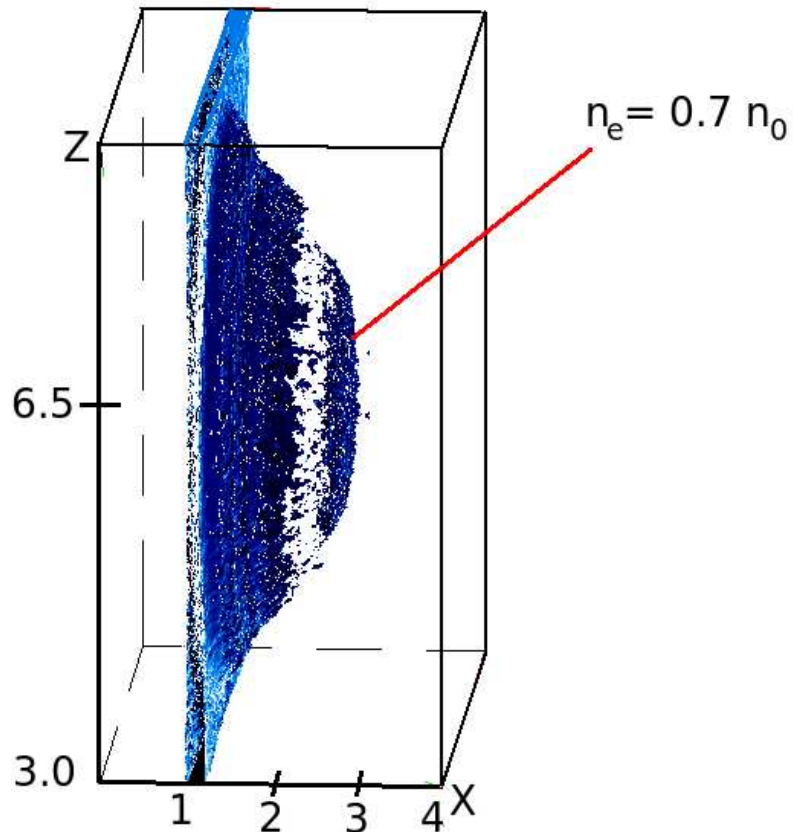
3D simulations of CP-RPA

182 PEs, $320 \times 1050 \times 1050$ grid, 80 points per λ
 $\sim 1.5 \times 10^9$ particles (27 per cell), 360 GBytes load



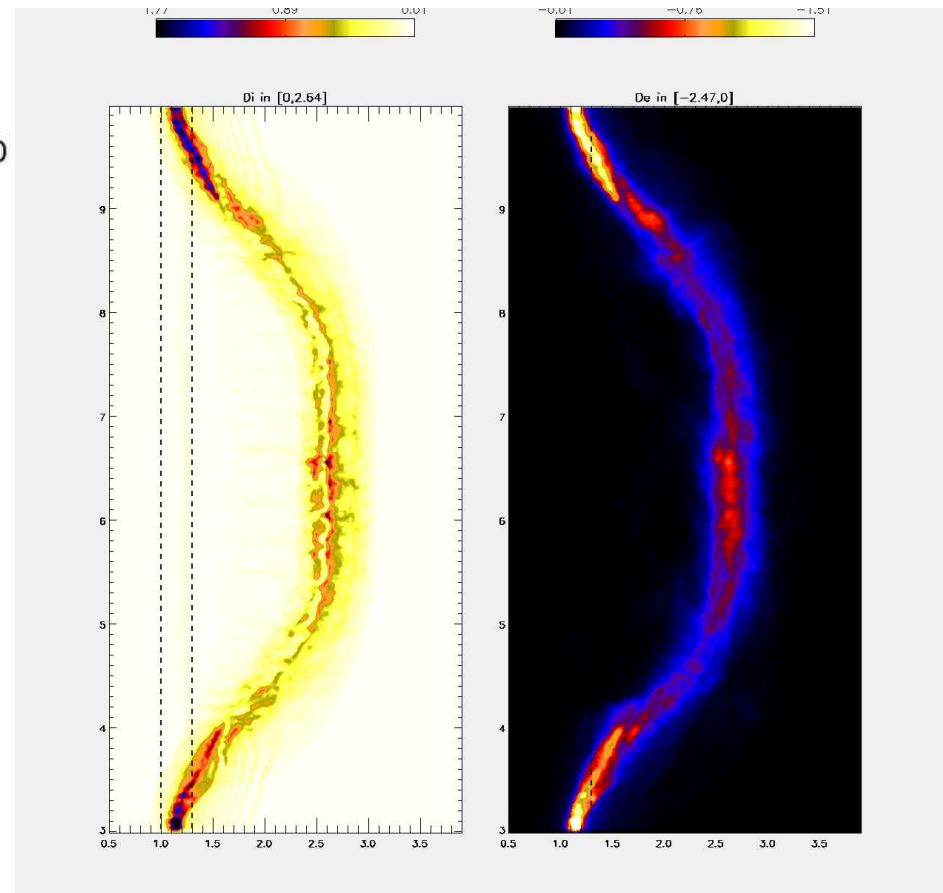
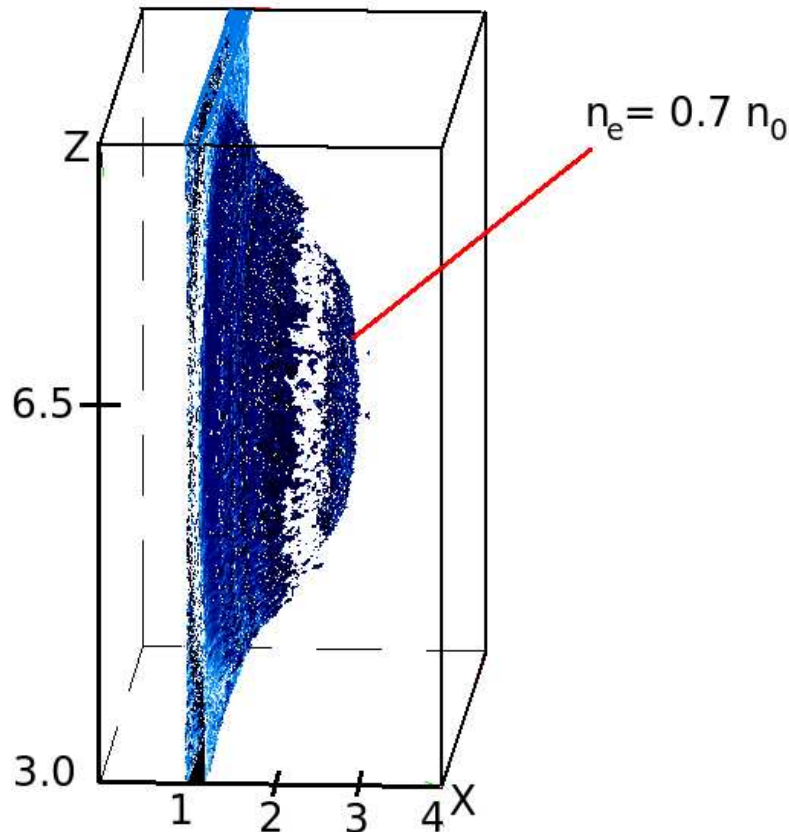
3D simulations of CP-RPA

182 PEs, $320 \times 1050 \times 1050$ grid, 80 points per λ
 $\sim 1.5 \times 10^9$ particles (27 per cell), 360 GBytes load



3D simulations of CP-RPA

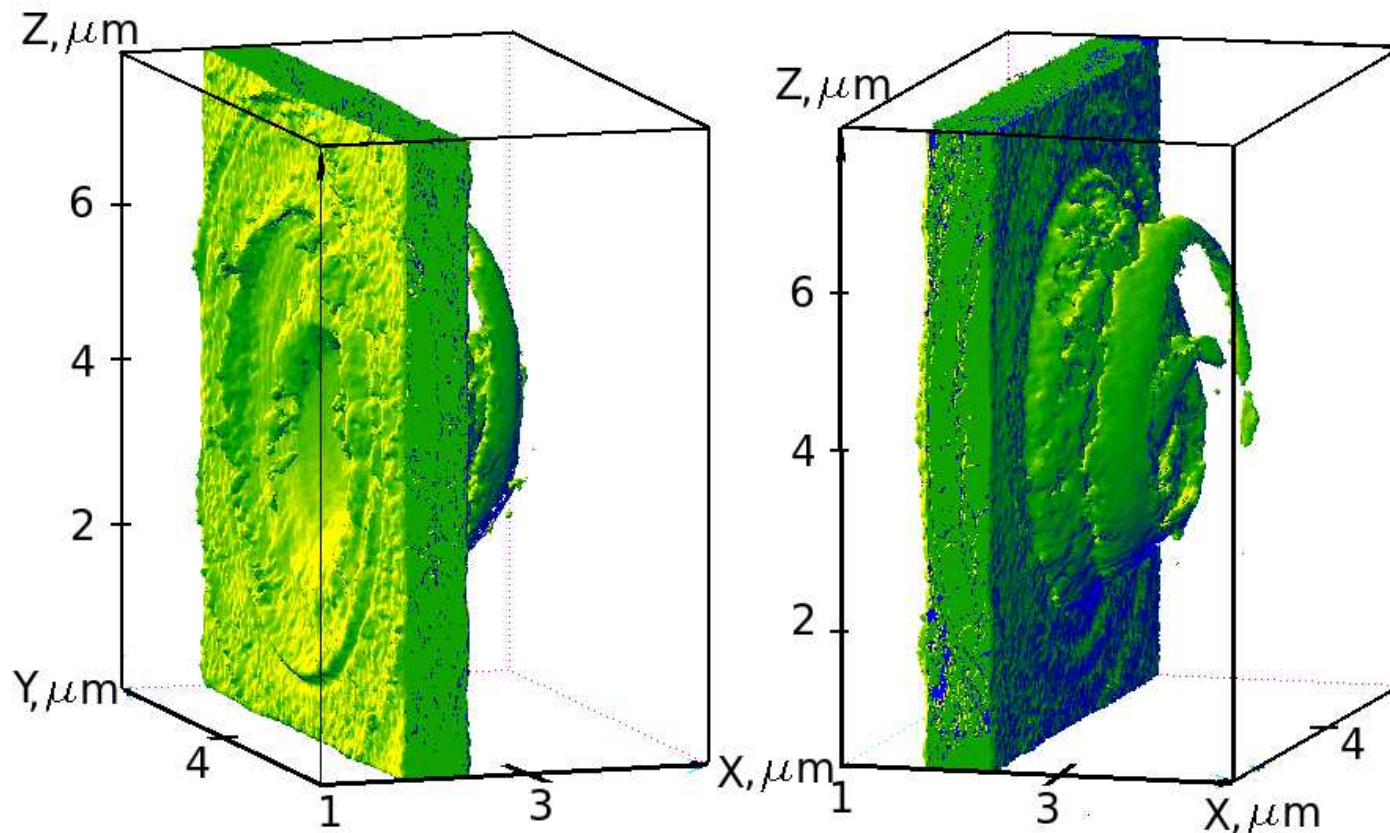
182 PEs, $320 \times 1050 \times 1050$ grid, 80 points per λ
 $\sim 1.5 \times 10^9$ particles (27 per cell), 360 GBytes load



3D simulations of CP-RPA

182 PEs, $320 \times 1050 \times 1050$ grid, 80 points per λ
 $\sim 1.5 \times 10^9$ particles (27 per cell), 360 GBytes load

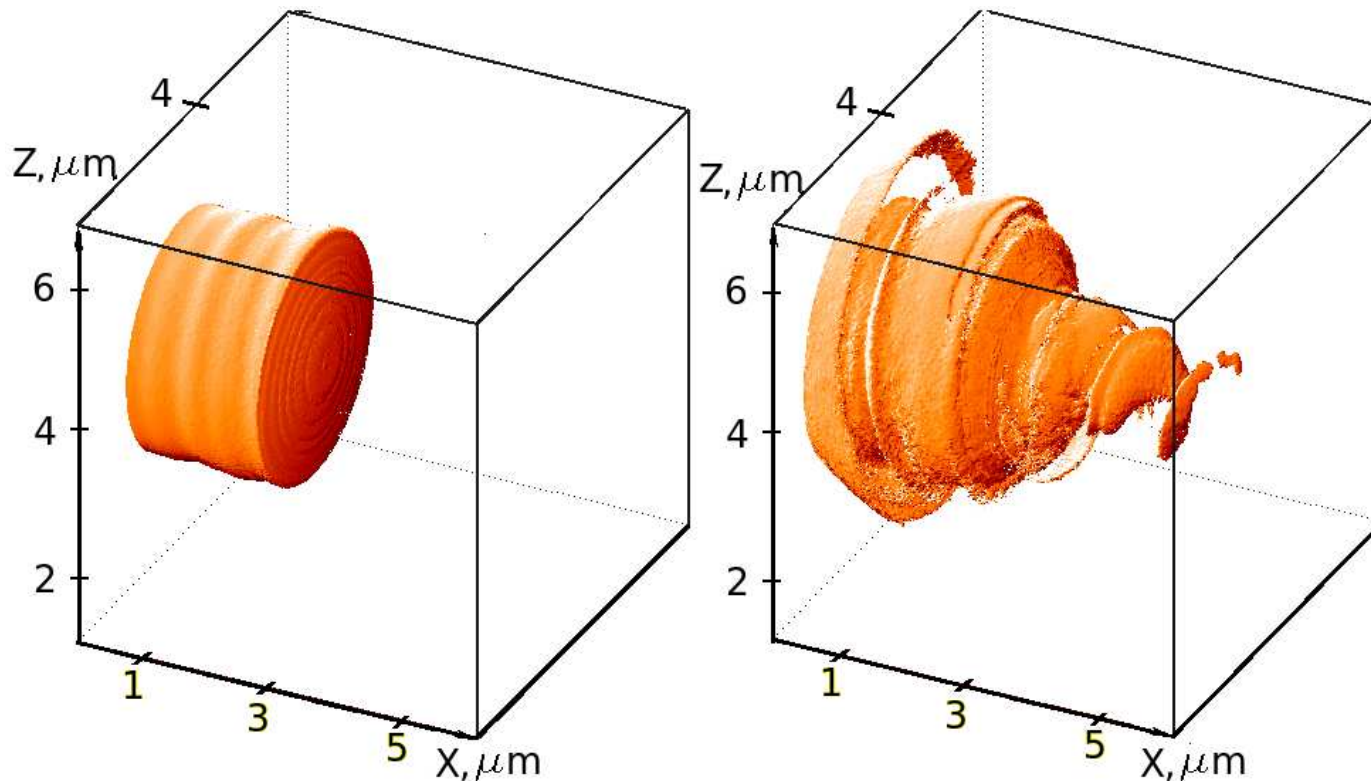
Electron density (rear and front views)



3D simulations of CP-RPA

182 PEs, $320 \times 1050 \times 1050$ grid, 80 points per λ
 $\sim 1.5 \times 10^9$ particles (27 per cell), 360 GBytes load

Electromagnetic energy density at two times



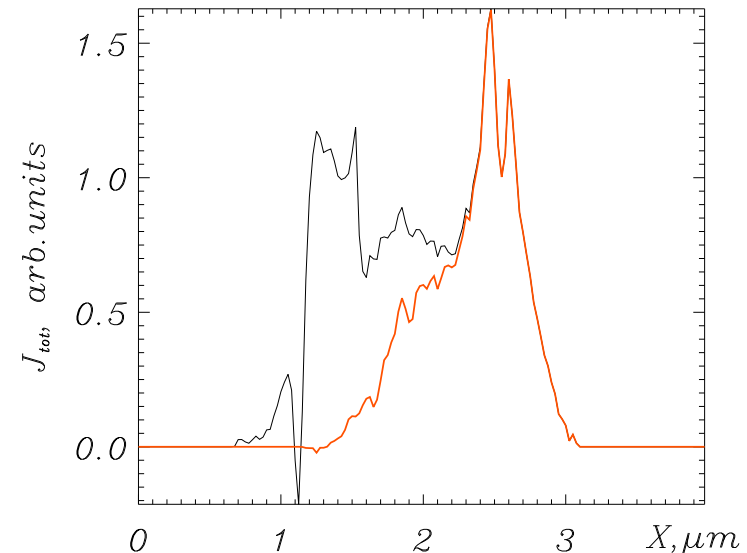
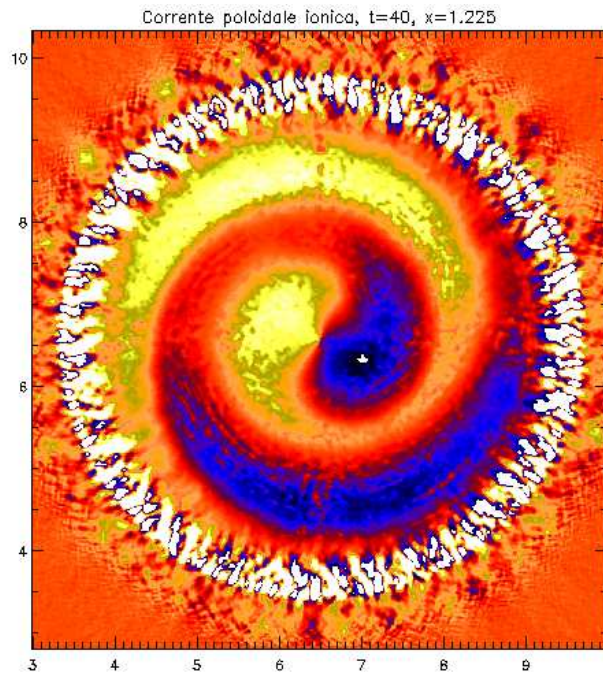
Angular momentum absorption

The total a.m. of plasma ions (electrons) is $\sim 4\%$ ($\sim 10^{-3}$) of the pulse a.m. – to be compared with a $\sim 10\%$ energy absorption.

Angular momentum absorption

The total a.m. of plasma ions (electrons) is $\sim 4\%$ ($\sim 10^{-3}$) of the pulse a.m. – to be compared with a $\sim 10\%$ energy absorption.

Angular momentum absorption is confirmed by integrating the azimuthal ion current ($J_{i,\phi}$) over the transverse plane (y, z)



Integrated ion current $J_{i,\phi}(x)$,
black line: all r , red line: $r < 2.5\lambda$,
 $r = \sqrt{y^2 + z^2}$.

Conclusions

- Laser-plasma physics is experiencing a very active growth: strong interplay between theory, experiment, and numerical simulations

Conclusions

- Laser-plasma physics is experiencing a very active growth: strong interplay between theory, experiment, and numerical simulations
- “*Plasma physics is (just) waiting for bigger computers*” – access to supercomputing resources is vital for this research

Conclusions

- Laser-plasma physics is experiencing a very active growth: strong interplay between theory, experiment, and numerical simulations
- “*Plasma physics is (just) waiting for bigger computers*” – access to supercomputing resources is vital for this research
- Strong interest by our group in maintaining its long-term activity at CINECA and in other projects

Conclusions

- Laser-plasma physics is experiencing a very active growth: strong interplay between theory, experiment, and numerical simulations
- “*Plasma physics is (just) waiting for bigger computers*” – access to supercomputing resources is vital for this research
- Strong interest by our group in maintaining its long-term activity at CINECA and in other projects
- Thanks to D. Bauer, C. Benedetti, M. Borghesi, F. Cattani, F. Ceccherini, F. Cornolti, S. Kar, F. Pegoraro, L. Romagnani (et al) for discussions, support and many other things, and to the CINECA staff for their help

Conclusions

- Laser-plasma physics is experiencing a very active growth: strong interplay between theory, experiment, and numerical simulations
- “*Plasma physics is (just) waiting for bigger computers*” – access to supercomputing resources is vital for this research
- Strong interest by our group in maintaining its long-term activity at CINECA and in other projects
- Thanks to D. Bauer, C. Benedetti, M. Borghesi, F. Cattani, F. Ceccherini, F. Cornolti, S. Kar, F. Pegoraro, L. Romagnani (et al) for discussions, support and many other things, and to the CINECA staff for their help
- Would you like to see it again?
www.df.unipi.it/~macchi/talks.html

EXTRA SLIDES

Mathematical model

Mathematical model

- Vlasov + Maxwell equations

Mathematical model

- Vlasov + Maxwell equations

$$\frac{\partial f_{i,e}}{\partial t} + \vec{v} \frac{\partial f_{i,e}}{\partial \vec{r}} + \vec{F}_{i,e} \frac{\partial f_{i,e}}{\partial \vec{p}} = 0, \text{ with } \vec{F}_{i,e} = q_{i,e} \left(\vec{E} + \vec{v} \times \vec{B} \right),$$

$$\text{rot } \vec{B} = \vec{j} + \frac{\partial \vec{E}}{\partial t}, \quad \text{rot } \vec{E} = -\frac{\partial \vec{B}}{\partial t}, \quad \text{div } \vec{E} = \rho, \quad \text{div } \vec{B} = 0$$

Mathematical model

- Vlasov + Maxwell equations

$$\frac{\partial f_{i,e}}{\partial t} + \vec{v} \frac{\partial f_{i,e}}{\partial \vec{r}} + \vec{F}_{i,e} \frac{\partial f_{i,e}}{\partial \vec{p}} = 0, \text{ with } \vec{F}_{i,e} = q_{i,e} \left(\vec{E} + \vec{v} \times \vec{B} \right),$$

$$\text{rot } \vec{B} = \vec{j} + \frac{\partial \vec{E}}{\partial t}, \quad \text{rot } \vec{E} = -\frac{\partial \vec{B}}{\partial t}, \quad \text{div } \vec{E} = \rho, \quad \text{div } \vec{B} = 0$$

dimensionless parameters:

Mathematical model

- Vlasov + Maxwell equations

$$\frac{\partial f_{i,e}}{\partial t} + \vec{v} \frac{\partial f_{i,e}}{\partial \vec{r}} + \vec{F}_{i,e} \frac{\partial f_{i,e}}{\partial \vec{p}} = 0, \text{ with } \vec{F}_{i,e} = q_{i,e} \left(\vec{E} + \vec{v} \times \vec{B} \right),$$

$$\text{rot} \vec{B} = \vec{j} + \frac{\partial \vec{E}}{\partial t}, \quad \text{rot} \vec{E} = -\frac{\partial \vec{B}}{\partial t}, \quad \text{div} \vec{E} = \rho, \quad \text{div} \vec{B} = 0$$

dimensionless parameters:

$$\lambda, t_0 = 2\pi c/\omega_0, E_0 = m_e c \omega_0 / (2\pi e), n_0 = m_e \omega_0^2 / 16\pi^3 e^2$$

Mathematical model

- Vlasov + Maxwell equations

$$\frac{\partial f_{i,e}}{\partial t} + \vec{v} \frac{\partial f_{i,e}}{\partial \vec{r}} + \vec{F}_{i,e} \frac{\partial f_{i,e}}{\partial \vec{p}} = 0, \text{ with } \vec{F}_{i,e} = q_{i,e} \left(\vec{E} + \vec{v} \times \vec{B} \right),$$

$$\text{rot} \vec{B} = \vec{j} + \frac{\partial \vec{E}}{\partial t}, \quad \text{rot} \vec{E} = -\frac{\partial \vec{B}}{\partial t}, \quad \text{div} \vec{E} = \rho, \quad \text{div} \vec{B} = 0$$

dimensionless parameters:

$$\lambda, t_0 = 2\pi c/\omega_0, E_0 = m_e c \omega_0 / (2\pi e), n_0 = m_e \omega_0^2 / 16\pi^3 e^2$$

- Charge and current density

Mathematical model

- Vlasov + Maxwell equations

$$\frac{\partial f_{i,e}}{\partial t} + \vec{v} \frac{\partial f_{i,e}}{\partial \vec{r}} + \vec{F}_{i,e} \frac{\partial f_{i,e}}{\partial \vec{p}} = 0, \text{ with } \vec{F}_{i,e} = q_{i,e} \left(\vec{E} + \vec{v} \times \vec{B} \right),$$

$$\text{rot} \vec{B} = \vec{j} + \frac{\partial \vec{E}}{\partial t}, \quad \text{rot} \vec{E} = -\frac{\partial \vec{B}}{\partial t}, \quad \text{div} \vec{E} = \rho, \quad \text{div} \vec{B} = 0$$

dimensionless parameters:

$$\lambda, t_0 = 2\pi c/\omega_0, E_0 = m_e c \omega_0 / (2\pi e), n_0 = m_e \omega_0^2 / 16\pi^3 e^2$$

- Charge and current density

$$\vec{j} = \sum_{i,e} q_{i,e} \int f_{i,e} \vec{v} d\vec{v}, \quad \rho = \sum_{i,e} q_{i,e} \int f_{i,e} d\vec{v}$$

Mathematical model

- Vlasov + Maxwell equations

$$\frac{\partial f_{i,e}}{\partial t} + \vec{v} \frac{\partial f_{i,e}}{\partial \vec{r}} + \vec{F}_{i,e} \frac{\partial f_{i,e}}{\partial \vec{p}} = 0, \text{ with } \vec{F}_{i,e} = q_{i,e} \left(\vec{E} + \vec{v} \times \vec{B} \right),$$

$$\text{rot} \vec{B} = \vec{j} + \frac{\partial \vec{E}}{\partial t}, \quad \text{rot} \vec{E} = -\frac{\partial \vec{B}}{\partial t}, \quad \text{div} \vec{E} = \rho, \quad \text{div} \vec{B} = 0$$

dimensionless parameters:

$$\lambda, t_0 = 2\pi c/\omega_0, E_0 = m_e c \omega_0 / (2\pi e), n_0 = m_e \omega_0^2 / 16\pi^3 e^2$$

- Charge and current density

$$\vec{j} = \sum_{i,e} q_{i,e} \int f_{i,e} \vec{v} d\vec{v}, \quad \rho = \sum_{i,e} q_{i,e} \int f_{i,e} d\vec{v}$$

$$\vec{p} = m\gamma\vec{v} - \text{particle momenta with } \gamma = (1 - v^2)^{-1/2}$$

Realisation

 PIC

Realisation

- PIC

Lee lattice for electromagnetic fields

Realisation

- PIC

Lee lattice for electromagnetic fields

Boris algorithm for equations of motion

Realisation

- PIC

Lee lattice for electromagnetic fields

Boris algorithm for equations of motion

“Exact charge conservation” – continuity equation is exactly fulfilled on the grid

Realisation

- PIC

Lee lattice for electromagnetic fields

Boris algorithm for equations of motion

“Exact charge conservation” – continuity equation is exactly fulfilled on the grid

- Cartesian geometry

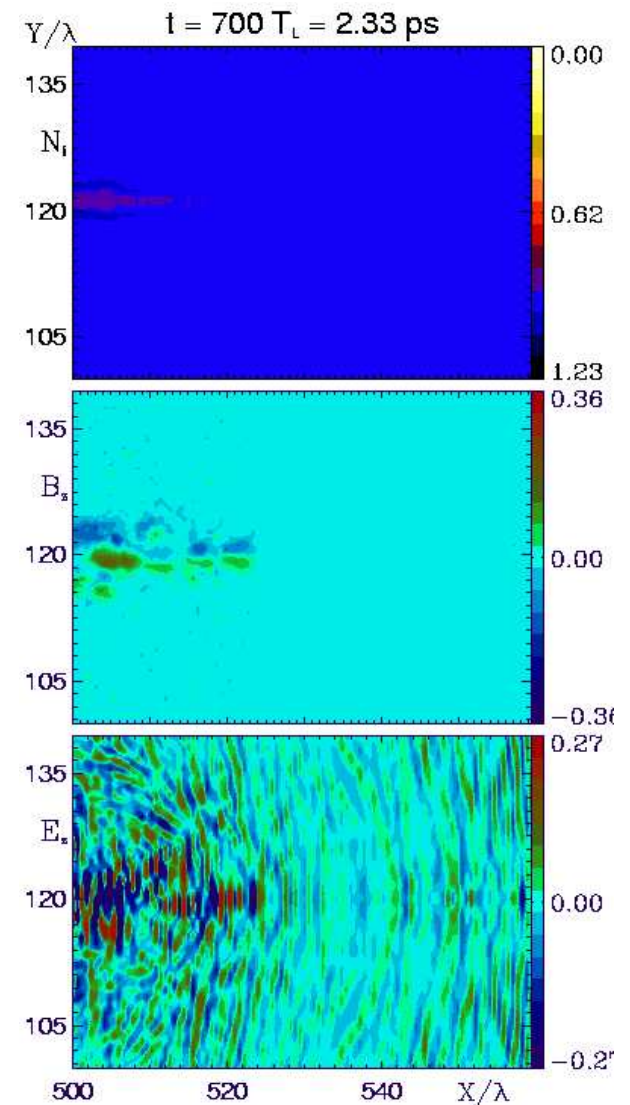
Evolution of field structures

Evolution of field structures

Pattern of standing “cavitons” grow inside low-density channels (due to the trapping of low-frequency light?)

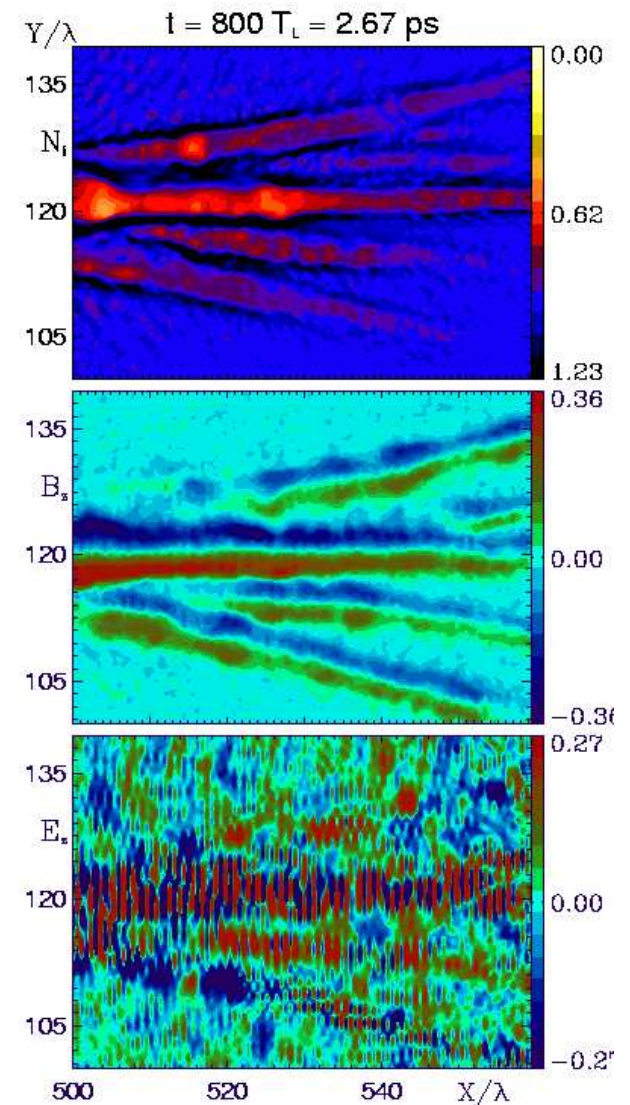
Evolution of field structures

Pattern of standing “cavitons” grow inside low-density channels (due to the trapping of low-frequency light?)



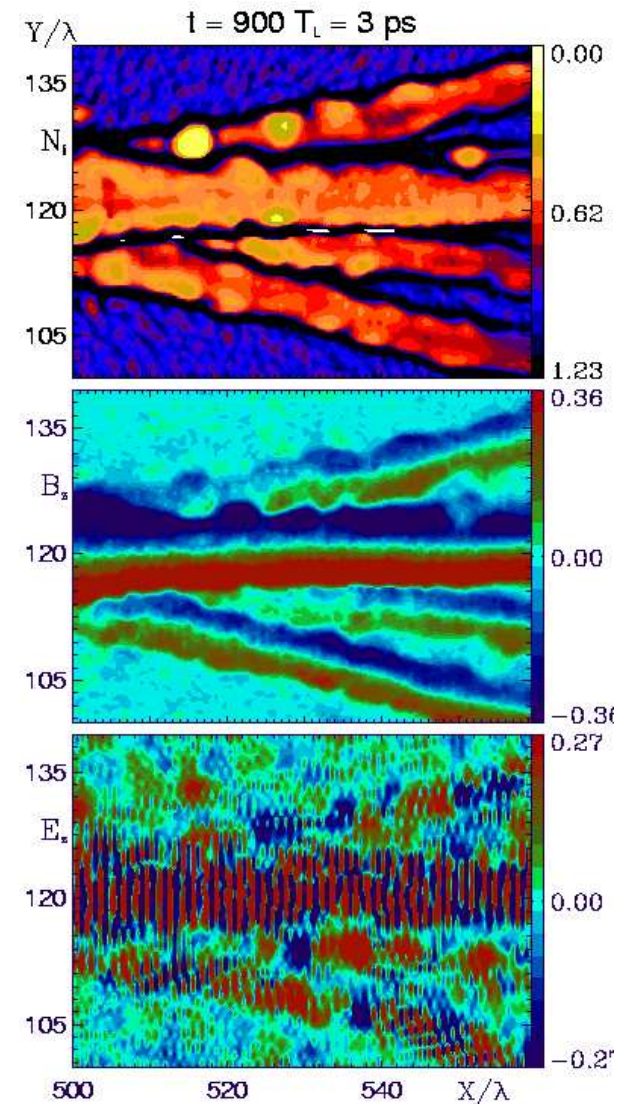
Evolution of field structures

Pattern of standing “cavitons” grow inside low-density channels (due to the trapping of low-frequency light?)



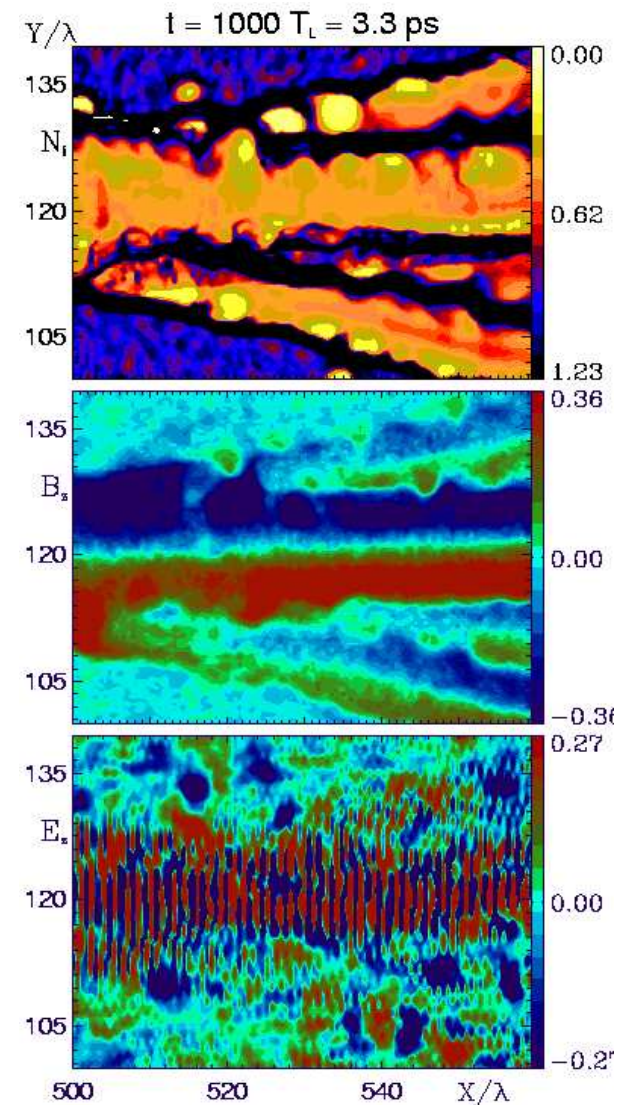
Evolution of field structures

Pattern of standing “cavitons” grow inside low-density channels (due to the trapping of low-frequency light?)



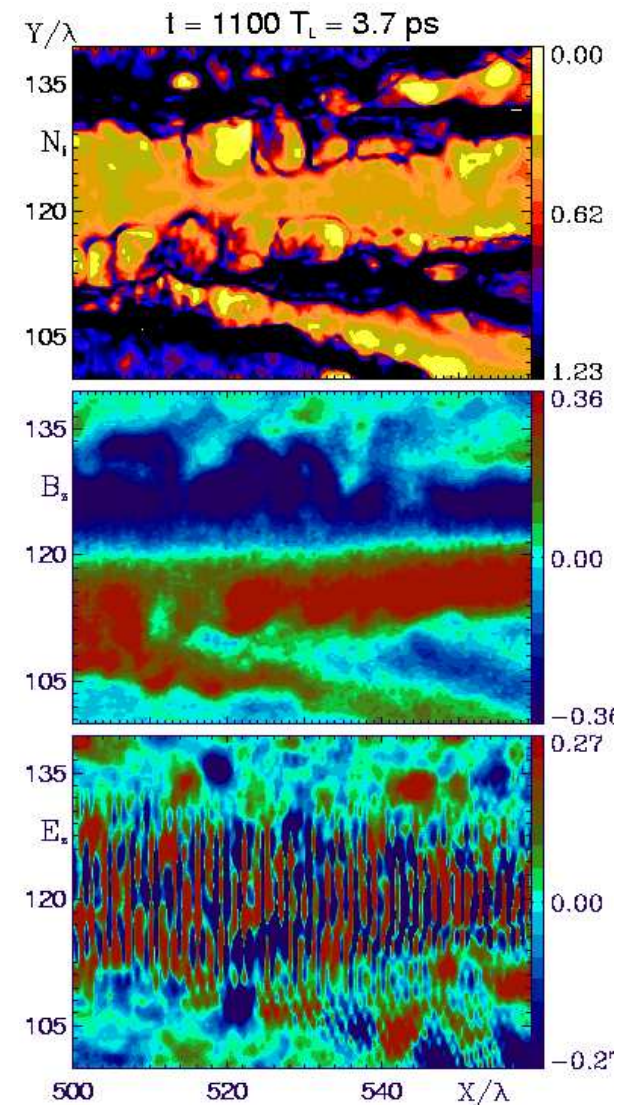
Evolution of field structures

Pattern of standing “cavitons” grow inside low-density channels (due to the trapping of low-frequency light?)



Evolution of field structures

Pattern of standing “cavitons” grow inside low-density channels (due to the trapping of low-frequency light?)



Evolution of field structures

Pattern of standing “cavitons” grow inside low-density channels (due to the trapping of low-frequency light?)

Comparison with experiments, based on reconstruction of Proton Imaging data by computing probe particles deflection in the slowly varying field patterns, is very promising

[A.Bigongiari, Thesis, Pisa, 2008].

